


Review

# A Review of Imaging Methods and Recent Nanoparticles for Breast Cancer Diagnosis

Fahimeh Aminolroayaei <sup>1</sup>, Saghar Shahbazi-Gahrouei <sup>2</sup>, Amir Khorasani <sup>1</sup> and Daryoush Shahbazi-Gahrouei <sup>1,\*</sup> 

<sup>1</sup> Department of Medical Physics, School of Medicine, Isfahan University of Medical Sciences, Isfahan 81746-73461, Iran; aminolroayaeif@gmail.com (F.A.); a.khorasani@resident.mui.ac.ir (A.K.)

<sup>2</sup> School of Medicine, Isfahan University of Medical Sciences, Isfahan 81746-73461, Iran; saghar.shahbazi73@gmail.com

\* Correspondence: shahbazi@med.mui.ac.ir; Tel.: +98-31-37929095; Fax: +98-31-36688597

**Abstract:** Breast cancer is the foremost common cause of death in women, and its early diagnosis will help treat and increase patients' survival. This review article aims to look at the studies on the recent findings of standard imaging techniques and their characteristics for breast cancer diagnosis as well as on the recent role of nanoparticles (NPs) that are used for breast cancer detection. Herein, a search was performed in the literature through scientific citation websites, including Google Scholar, PubMed, Scopus, and Web of Science, until May 2023. A comprehensive review of different imaging modalities and NPs for breast cancer diagnosis is given, and the successes, challenges, and limitations of these methods are discussed.

**Keywords:** breast cancer; diagnostic; mammography; ultrasound; magnetic resonance imaging



**Citation:** Aminolroayaei, F.; Shahbazi-Gahrouei, S.; Khorasani, A.; Shahbazi-Gahrouei, D. A Review of Imaging Methods and Recent Nanoparticles for Breast Cancer Diagnosis. *Information* **2024**, *15*, 10. <https://doi.org/10.3390/info15010010>

Academic Editor: Gholamreza Anbarjafari (Shahab)

Received: 10 December 2023

Revised: 19 December 2023

Accepted: 20 December 2023

Published: 22 December 2023



**Copyright:** © 2023 by the authors. Licensee MDPI, Basel, Switzerland. This article is an open access article distributed under the terms and conditions of the Creative Commons Attribution (CC BY) license (<https://creativecommons.org/licenses/by/4.0/>).

## 1. Introduction

Breast cancer (BC) has the highest incidence rate and is the foremost common cause of death in women. BC is about 100 times more common in women than in men. The risk factors for BC are alcohol intake, body mass index, hormone replacement therapy with estrogen and progesterone, radiation exposure, early and late menarche, and late age in first childbirth. Also, current age (increasing age increases the risk of developing BC), history of BC, breast biopsy, cytology, family history, inherited mutation in the BRCA1 or BRCA2 gene [1], and the risk of BC and interval cancers is four to six times higher in women with very dense breast (DB) tissue than in those with fatty breasts [2]. Countries with an excellent human development index (HDI) have the highest incidence of BC due to obesity, physical inactivity, and alcohol consumption. Still, the mortality rate from BC is higher in countries with a small HDI, because in countries with an excellent HDI, patients have a higher socioeconomic status, are usually diagnosed earlier, and have more prolonged survival [3]. Recent advances in technology have transformed the landscape of cancer detection, with digital pathology emerging as a game-changer in the field of breast cancer detection and analysis [4]. Digital pathology is a dynamic, image-based environment that enables the acquisition, management, and interpretation of pathology information generated from a digitized glass slide. It leverages technologies such as whole-slide imaging (WSI), image analysis algorithms, machine learning, and artificial intelligence (AI) to enhance the accuracy and efficiency of pathological examinations [5,6]. In the context of breast cancer, digital pathology offers several advantages over traditional pathology. It allows for high-resolution imaging of tissue samples, enabling pathologists to examine cells and tissues in unprecedented detail. It also facilitates quantitative analysis, providing objective and reproducible measurements that can be crucial in determining the stage and grade of the cancer. Moreover, digital pathology can harness the power of AI to automate the identification of cancerous cells, potentially increasing the speed of diagnosis while reducing the workload for pathologists [4,7]. However, the implementation of digital

pathology is not without its challenges. Issues such as data management, interoperability, and the validation of digital pathology systems and AI algorithms must be addressed. Additionally, there are ethical and legal considerations regarding patient privacy and the use of digital images.

Breast imaging is employed for cancer detection, diagnosis, and clinical management [8]. Imaging can detect approximately 85% of BC cases [9]. Medical imaging methods for BC diagnosis, as indicated in Figure 1, are categorized into three main imaging methods: (1) mammography (MG) and its derivatives, including full-field digital mammography (FFDM) or digital mammography (DM), tomosynthesis (TS), 3D mammography, digital breast tomosynthesis (DBT), and contrast-enhanced mammography (CEM); (2) ultrasound (US) imaging or sonography due to its application in soft tissue; and (3) magnetic resonance imaging (MRI) and its derivatives, including dynamic contrast-enhanced breast MRI (DCE-MRI), diffusion-weighted imaging (DWI), magnetic resonance spectroscopy (MRS), and magnetic resonance elastography (MRE). Each of these modalities has its advantages, successes, and limitations in BC diagnosis. These modalities have different imaging durations. Computed tomography (CT-Scan), with its rapid acquisition, proves indispensable in emergency scenarios, ensuring swift diagnostic assessments. Conversely, MR imaging, though providing detailed anatomical information, is associated with longer acquisition times, necessitating careful planning to optimize workflow. Ultrasound, characterized by its real-time capabilities, offers a quick and non-invasive option that is suitable for dynamic assessments and procedural guidance. Radiography, widely employed for its rapid image acquisition, stands out as an efficient choice in scenarios in which quick results are essential. Recognizing the distinctive duration characteristics of each modality becomes pivotal in clinical decision making, guiding the selection of the most appropriate imaging technique based on specific clinical requirements and urgency.

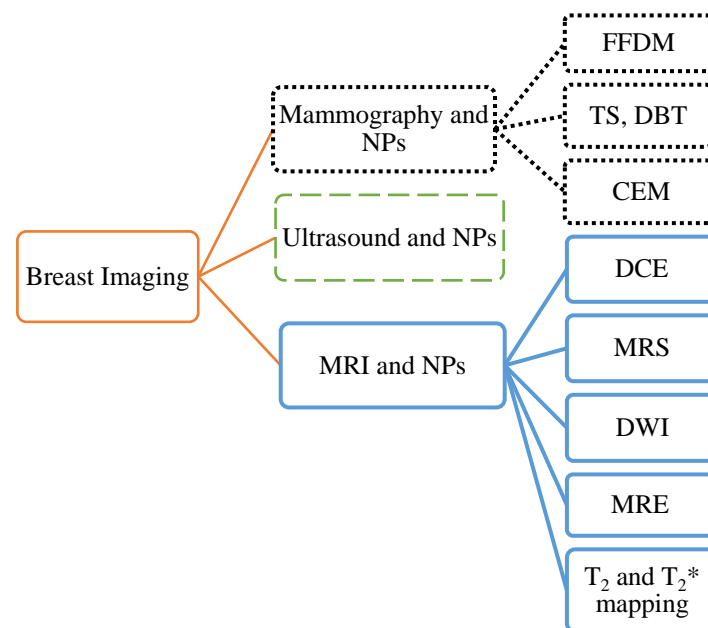


**Figure 1.** Common imaging modalities for BC diagnosis. Abbreviation: NPs: nanoparticles.

In recent years, nanoparticles have emerged as a promising tool for breast cancer detection. Nanoparticles are tiny particles that have unique physical and chemical properties due to their small size. They can be engineered to target specific cells and tissues in the body, including cancer cells. The use of nanoparticles for breast cancer detection offers several advantages, such as high sensitivity, specificity, and non-invasiveness. This topic has gained significant attention, and researchers are exploring different types of nanoparticles and their potential applications in breast cancer detection.

This review article aims to conduct comprehensive studies on the recent findings of standard imaging techniques and their characteristics for breast cancer diagnosis and to provide an overview of the recent role of nanoparticles in breast cancer detection.

## 2. Mammography (MG)

Mammography includes imaging the breast using low-energy X-rays, which detect BC, benign tumors, and cysts before detection by touch. It has a sensitivity or true positive of about 75%, but in middle-aged people with higher breast tissue density, the sensitivity decreases to about 50% [10]. MG has some advantages. First, it is the gold standard for diagnosing BC patients. Second, MG is suitable as a screening method for disease prevention, as it helps in the finding and removal of premalignant precursors of cancer and in the early detection of cancer for BC [11]. It is demonstrated that the risk of death from BC in women who are invited for screening is reduced by 22% compared to women who are not invited [12].

It should be noted that screening methods such as DM, DBT, and CEM should be considered to have small or negligible risks of radiation-induced cancer or death. Still, screening methods with radionuclide injection have significantly higher cancer risks unless efficient detection systems and prescribed dose reductions are used [13]. Third, MG can find mammary gland calcification. It is known that approximately 25 to 43% of non-palpable cancers are detected in MG due to microcalcifications [14]. Of course, MG is not suitable for people under 40 years of age, it cannot be undertaken more than twice a year [15], and it is limited in imaging DB tissue [16].

### 2.1. Full-Field Digital Mammography (FFDM)

Mammography can be performed using screen film (SFM) or DM. The advantages of SFM include its high contrast and the high spatial resolution of about 15–20-line pairs/mm. Limitations include the limited dynamic range, and film display characteristics such as brightness and contrast are fixed after the film is developed in a chemical processor. Compared to SFM, DM has advantages such as a more comprehensive dynamic range and better contrast resolution, especially for DB tissue. It is also possible to use post-processing on the digital image to increase the quality of the image [17]. It has been found that DM has similar accuracy, specificity, and sensitivity as SFM in diagnosing BC [18]. A comparison of SFM and DM showed that digital MG has a statistically higher cancer detection rate, an increase in recall and false positive screens, and no effect on interval cancer rates [19]. Digital mammography is also more accurate in women below 50 years of age, those with DB, and premenopausal or postmenopausal women [20]. DM has a lower average radiation dose than SFM without compromising diagnostic accuracy [20].

Posso et al. [21] led an investigation on reducing the masking effect of DM breast density compared to SFM and improving cancer detection, especially in women with high DB [22]. The study showed that high breast density harms DM, and its sensitivity and positive predictive value decrease. Of course, the authors noted that although sensitivity decreases, cancer detection increases.

Although FFDM is the gold standard for effective screening and diagnosis of BC in the early stages because of its low cost, fast speed, and non-invasive technique, it leads to false positives and negatives due to overlapping breast tissue. Therefore, DBT improves cancer detection rates [23], because DBT can reduce the overlap of normal breast parenchyma and reveal clinically obscure lesions [24]. One of the differences between FFDM and DBT is the kVp values used. In MG, the kVp is chosen to provide high contrast, but contrast is not required in tomosynthesis, because the DBT information is reconstructed in the images. For this reason, more penetrating X-ray photons are used to achieve a high signal-to-noise ratio and increase patients' radiation doses [25].

## 2.2. Digital Breast Tomosynthesis (DBT)

Digital breast tomosynthesis is a 3D mammogram with multiple projections rotating through an arc of 15 and 60 degrees in a plane parallel to the chest wall. It should be noted that by sampling a wide angular range, tomosynthesis has advantages such as the obtainment of more information, superior depth resolution, and better contrast than narrow-angle sampling. However, patient movement may occur due to the longer imaging duration [26].

Compared to MG, DBT shows an increase in cancer detection and a decrease in the recall rate, but it is associated with an increase in the radiation dose [27]. Østerås et al. [28] showed that compared to DM, DBT can identify more cancers in all density and age groups, and false positive findings due to asymmetric density are less frequent. Another comparison between DBT and FFDM showed that DBT identified more cancers of all sizes, grades, and hormone receptor statuses, with or without node involvement. Similarly, more cancers were detected with DBT than FFDM regardless of age group, density classification, or the presence or absence of prior examination [29].

In a study, Lee et al. [30] showed that DBT might be more effective in BC screening in patients with DB. A comparison of DBT and FFDM has demonstrated that invasive lobular carcinoma, lower histologic-grade HER-2-negative lesions, lesions presenting as masses, or lesions with architectural distortion are better characterized in DBT images. However, DBT has limitations due to surrounding glandular tissue in DB, and these types of cancers are ignored in both methods. One of the essential issues in reducing the risk of local tumor recurrence is the ability to predict the tumor margin. Still, FFDM provides a two-dimensional image, so it cannot anticipate this. Romanucci G et al.'s work [31] confirmed the ability of DBT to better visualize the lesion margin.

Heindel et al. and You et al. [32,33] compared DM and DBT with synthetic mammography (SM gives a virtual 2D MG image obtained from DBT, which looks similar to that from FFDM). According to their analysis, it was found that the detection rate of invasive BC is significantly higher with DBT with SM. In another study, Choi et al. [34] showed that SM might be slightly more sensitive than DM for detecting and characterizing microcalcifications. Also, SM plus DBT can replace DM plus DBT for detecting microcalcifications. It was also shown that DBT with SM is a better method than FFDM for detecting mass, calcification, and asymmetry [35], which is shown in Figure 2.

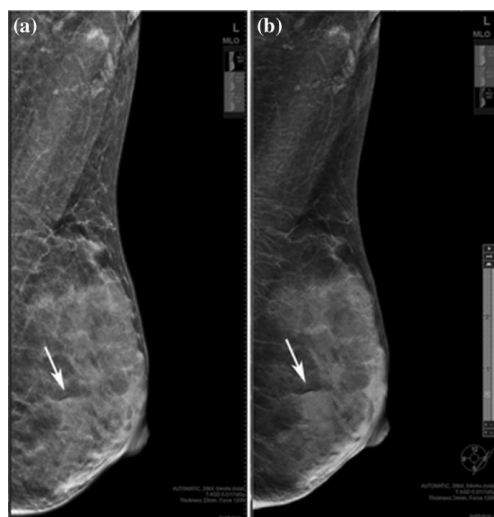


**Figure 2.** A 36-year-old woman with a fibroadenoma in the left breast. (a) FFDM and (b) SM mediolateral oblique images. Rows indicate benign lesion, which is asymmetric on SM and an obscured mass on DBT. “Reprinted with permission from Ref. [35]. 2019, Springer”. More details on “Copyright and Licensing” are available via the following link: <https://link.springer.com/article/10.1007/s12282-019-00992-1> (accessed on 1 December 2023).

Furthermore, DBT increases cancer detection rates, reduces recall rates compared to FFDM, and improves sensitivity and specificity. DBT with SM (instead of FFDM) has a radiation dose similar to that of FFDM alone [36]. A comparison between the image quality of SM and DM demonstrated that the spatial resolution and contrast detail curve in SM is lower than that in DM. Still, SM has some advantages, like decreasing the radiation dose, reducing imaging time [37], and improving diagnostic efficacy for detecting malignant breast lesions [33]. Theoretically, DBT may show only a few calcifications of a clinically significant micro-calcification cluster, but FFDM has a higher sensitivity in detecting and characterizing calcifications. In the study of Murakami et al. [38], it was found that SM can compensate for the disadvantages of DBT in underestimating calcification.

Adding DBT to FFDM has advantages such as increased sensitivity, specificity, and positive predictive value, reducing the false positive rate in diagnostic and screening cases and increasing the cancer detection rate [39]. Skaane et al.'s study has determined that adding DBT to DM significantly increases sensitivity and specificity. Though using SM instead of DM in combination with DBT causes a slight change in sensitivity or specificity, it can be a suitable alternative to DM when using DBT [40]. The results of a study by Yi et al. [41] showed that the tumor visibility and diagnostic performance of DBT added to FFDM in the evaluation of women with T<sub>1</sub> non-calcified invasive BC depend on the composition of the breast and the probability of failed diagnosis in both DBT and FFDM images in small isodense non-calcified cancer that is in the tissue, where dense fibro glandular glands are hidden. Therefore, complementary imaging other than DBT should be considered for screening women with very DB. A study by Alabousi et al. showed that combined DBT and DM or combined DBT and SM resulted in higher cancer detection rates, higher invasive cancer detection rates, and higher positive predictive value than DM alone. The combination of DBT and SM reduced the recall rate for additional imaging and biopsy. However, DBT alone has no advantage compared to DM alone [42]. Another study showed that the diagnostic accuracy and sensitivity of DBT plus SM are higher than that of FFDM alone, and its recall rate for DB is lower than that for FFDM [43].

Although DBT combined with DM can increase diagnostic accuracy and reduce the recall rate, it leads to more extended time necessary for interpretation and a higher radiation dose [44,45] due to two separate acquisitions. Hence, synthesized mammography (SM) reconstructed from DBT images can be a potential alternative to DM, which leads to a significant reduction in the total radiation dose [25] without compromising diagnostic accuracy [46].

### 2.3. Contrast-Enhanced Mammography (CEM)

Contrast-enhanced mammography is an imaging procedure that combines digital MG with copper filtration and additional software to perform dual-energy imaging at about 26–33 kVp and 44–50 kVp and administer intravenous nonionic low-osmolar iodinated contrast media [47]. The reason for using contrast media in CEM is the low difference in the absorption of X-rays between the tissues and, thus, the similarity of the image contrast of the tumor tissue compared to the glandular tissue in DB [48]. Rasouli et al. (47) recently demonstrated the advantages of iodine nanoparticles compared to gold nanoparticles. In this study, they reported that iodine works better than gold nanoparticles, and the cytotoxicity of gold nanoparticles is higher than that of iodine. Therefore, it was stated that in general, iodine has a better performance than gold nanoparticles.

In CEM, two images of each view are obtained at two energy levels. The first image is a low-energy image that shows breast morphology and is equivalent to a standard 2D mammogram and another image provides low- and high-energy images showing areas of contrast absorption [49]. Imaging breast tissue with one direction of X-ray exposure is ineffective for BC detection. A dual-energy imaging technique can overcome this problem, resulting in a high dose. Li et al. [50] investigated the use of CEM with photon counting detectors (PCDs) using cadmium zinc telluride (CZT) and total variation (TV) denoising algorithms. The study showed that CEM with PCD can be used to solve the problem of

high doses in dual-energy imaging systems, and TV can improve the image quality for BC diagnosis.

The studies' results have shown that CEM's morphological and physiological information has higher sensitivity and specificity than DM alone. Also, CEM is significantly more sensitive and specific than MG alone and has sensitivity and specificity comparable to CE-MRI [51]. Another comparison of different imaging modalities for BC detection showed that FFDM and 3D tomosynthesis rely on subtle morphologic and density differences to detect BC, which can be obscured by dense glandular tissue overlap [52]. Sorin et al. showed that CEM is more sensitive than MG for BC detection, and it has higher diagnostic accuracy than MG alone and MG combined with US. However, CEM has less specificity than MG and, as a result, increases false positive findings and recall rates [53]. Sudhir et al. [54] compared DBT, SM, US, and CEM. According to their results, the sensitivity of CEM was significantly higher than that of SM, DBT, and DBT plus US. CEM also showed significantly higher specificity than SM and was comparable to DBT alone and DBT plus US. The authors stated that although CEM has higher sensitivity than DBT, the description of the margin and exact location of breast lesions is better evaluated in DBT.

Contrast-enhanced mammography in BC detection has advantages such as a performance similar to breast MRI, a cost identical to conventional MG, and time imaging similar to an abbreviated MRI protocol and inferior to MRI. Less time is needed by the radiologist to perform the procedure and interpret the findings [55,56]. As mentioned, the sensitivity and specificity of standard MG are affected by breast tissue density. The US depends on the operator's experience. Although MRI is the most sensitive breast imaging method, it has a high rate of false positive results. Therefore, Bozzini et al. [57] evaluated CEM in DB patients with histologically proven malignant breast lesions and compared its diagnostic performance with US, FFDM, and MRI. According to the study, CEM had a detection rate similar to US and MRI, and it was significantly higher than that of FFDM (Figure 3). Invasive tumor size obtained by CEM matched pathological data in 64.6% of lesions, similar to US and MRI but higher than FFDM.

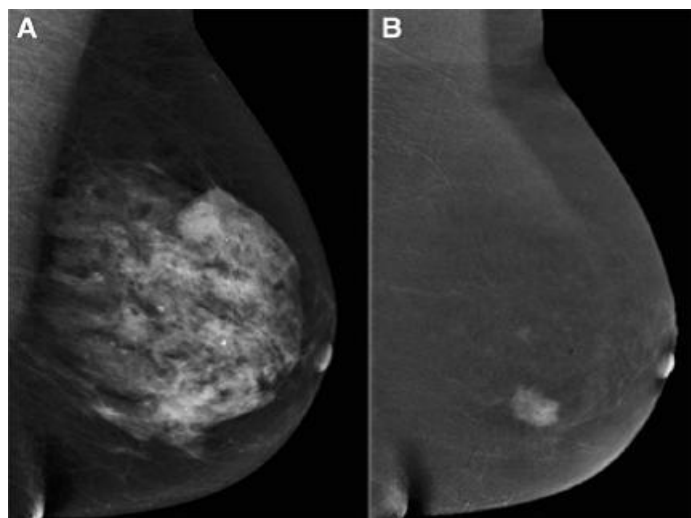


**Figure 3.** (A) FFDM showing a dense breast and (B) the same breast on CEM showing breast cancer [58]. “Reprinted with permission from Ref. [56]. 2020, Springer”. More details on “Copyright and Licensing” are available via the following link: <https://link.springer.com/article/10.1007/s10549-020-05881-2> (accessed on 1 December 2023).

In malignancies, the contrast agent is absorbed more than in normal tissue due to high angiogenesis. Therefore, methods such as DCE-MRI and CEM have been given attention. Contrast-enhanced mammography is superior to DM and DBT in terms of accuracy and is comparable to DCE-MRI in evaluating breast malignancy [58]. Based on Huang et al. [59],

benign and malignant lesions showed the highest contrast enhancement at 3 and 2 min, respectively. Therefore, to observe the maximum contrast enhancement of BC in CEM, 2 min is the best interval to differentiate between benign and malignant breast lesions.

About BC, it should be noted that not completely removing cancer cells leads to the creation of disease-resistant cells. These cells are undetectable and can unpredictably lead to recurrence and metastasis. Such drug resistance prevents anti-cancer treatments, so it is necessary to improve diagnostic methods [60]. Studies have been conducted that investigate the ability of different imaging methods in the diagnosis of residual disease. For example, the study of Molly P. Hogan et al. has shown that CEM is an acceptable alternative to breast MRI for the diagnosis of residual disease after neoadjuvant treatment [61].

Bicchierai et al. [62] investigated the potential of using CEM before surgery. The study showed the excellent diagnostic performance of CEM in the correct preoperative staging of BC. The authors stated that this method has a high sensitivity in the preoperative staging of BC compared to DM, even when combined with the US. They also noted that this method has a low rate of false positives and false negatives as a preoperative imaging method. In this study, false negative results were not cancers missed by CEM but cases with positive surgical specimen margins.

Despite all the mentioned advantages of CEM in patients with lesions, it is not suitable in patients with spreading of unifocal disease, ductal carcinoma in situ histotypes, lesion size less than 10 mm, and index lesion with micro-calcification [63]. This method also has some disadvantages, such as the need to inject contrast agents, which can lead to allergic reactions, and CEM-guided biopsy is unavailable. There may be a low rate of false positive and false negative results, and benign tissues can be associated with contrast enhancement, which leads to unnecessary imaging and biopsy [64]. CEM does not have sufficient sensitivity to detect poorly advanced cancers. In addition, it does not show cancers with increased parenchyma in the background or near the chest wall [51].

#### 2.4. Nanoparticles in Mammography

The use of nanoparticles (NPs) in medical imaging and mammography is fast becoming a key instrument in cancer detection and treatment. A large and growing body of literature has investigated the use of different NPs in mammography. Surveys such as that conducted by Naha et al. [65] have shown that gold–silver alloy NPs (GSAN) can be used as a contrast agent for cancer detection with dual-energy mammography and computed tomography (CT). It has been demonstrated that [66] a high biocompatibility of silver telluride NPs ( $\text{Ag}_2\text{Te}$  NPs) results in their use in mammography and as a CT contrast agent for cancer detection. Karunamuni et al. [67] found that silver NPs are an effective contrast agent for cancer detection and screening with dual-energy mammography. In a study that set out to increase the sensitivity and specificity of mammography for cancer detection, Cole et al. [68] found that bisphosphonate-functionalized gold NPs (BP-Au NPs) improved sensitivity and specificity for the detection of microcalcifications. In another study, Cole et al. [69] points out that BP-Au NPs can be used for dense mammary tissue imaging with high sensitivity and specificity.

### 3. Ultrasound Imaging (US)

Ultrasound is a screening method that does not require ionizing radiation or intravenous contrast. US has advantages such as its portability, lower cost than MG, and versatility. It is the perfect imaging tool for biopsy, as it distinguishes cystic masses from solid masses. Choudhery et al. [70] investigated the adequacy of the US to detect masses. According to their study, most masses recalled from DBT screening can be evaluated with just an US. A diagnostic MG should be performed if the recalled mass is not seen. A handheld US (HHUS) or an automatic breast US (ABUS) can be used [71]. Both have 100% sensitivity, and their specificity is 85% and 95%, respectively. One of the advantages of the automatic type is its higher diagnostic accuracy than the manual type [72], and it overcomes limitations such as being operator-dependent, time-consuming, and unrepeatably [73]. It

has been made clear that the US has low specificity and false positive risk [74], and a double reading of the ABUS can solve this problem. This was investigated in a study by Lee et al. [75]. The study showed that double reading could increase diagnostic efficiency and decrease false positives. The authors also stated that adding ABUS can improve the recall rate of FFDM and DBT screening. Based on a meta-analysis by Rupali et al. [76], the US has a sensitivity and specificity of 80.1% and 88.4% for BC diagnosis; hence, the authors showed that it incorporates a high potential for BC diagnosis and can be utilized as an early diagnosis tool. Even though the studies the authors checked were heterogeneous, this demonstrated a limited impact on their conclusions. In another study, Badu-Peprah et al. [77] showed that the sensitivity of the clinical diagnosis is 50.5%, MG 73.0%, and US 100%, and the specificity of MG and US is 80.0% and 80.4%, respectively. In this manner, they proposed that the US be utilized as the primary line of imaging for diagnosis. In addition, a study conducted by Harada-Shoji et al. [78] compared the sensitivity of MG and US and found that the sensitivity of MG and US alone is lower than the combined sensitivity of these methods, that is, if US is utilized as a supplement to MG, the sensitivity increases. In addition, the authors indicated that the adjuvant US increases the detection of early invasive cancers in dense and non-DB.

In a study by Yi et al. [79], the authors investigated the value of adding US after DM/DBT. According to their research, the addition of the US led to the detection of three extra cancers in 925 women with negative DM/DBT results, and all other cancers were detected in women with DB. Still, US screening in women with non-DB who experienced DM/DBT is useless. Another study compared the utilization of US after DM and after DMT in women with DB. This study showed no difference in diagnosis when US is utilized after DM or after DMT, and the utilization of DMT does not remove the additional US in women with DB [80]. Comparing CEM and US showed that axillary and lymph node lesions might not be seen in CEM, but the US can show these regions' anomalies [81]. Moreover, a study by Lu et al. [82] compared the performance of CEM and US in patients with DB. The sensitivity, specificity, positive predictive value, negative predictive value, and accuracy of CEM were 93.8%, 88.1%, 88.2%, 93.7%, and 90%, respectively, and 90.6%, 82.1%, 82.9%, 90.8%, and 86.3% for the US. The authors stated that the ability of the US to detect benign lesions is higher than that of CEM, and misdiagnosis with CEM can delay the treatment of benign lesions. A comparison between MG and US also showed that MG is not a viable diagnostic method for DB [83], because dense tissue and BC are seen as white in MG, whereas in US, dense tissue is echogenic, and BC is hypoechoic (Figure 4). It has been found that the addition of US screening can increase the BC detection rate by 1.9–4.2% [84].

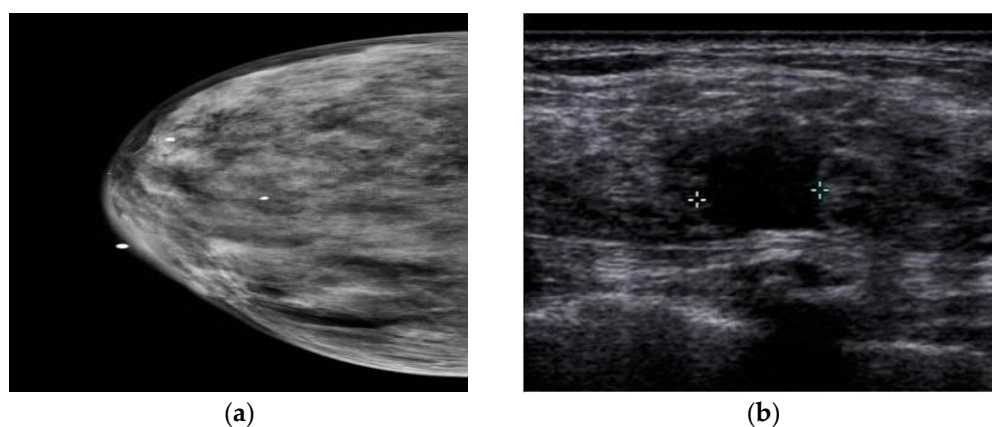


**Figure 4.** (a) DB is white in MG like BC. (b) DF is echogenic, but BC is hypoechoic in US [84]. More details on “Copyright and Licensing” are available via the following link: Creative Commons—Attribution 4.0 International—CC BY 4.0.



The drawbacks of the US profoundly depend on the experience of the radiologist [85]. It has unsatisfactory false positives and false negatives in asymptomatic women [86]. The trouble in recognizing between a cyst and a solid tumor can be remedied by Doppler and Power Doppler methods [87]. In women with a background of BC, there is a possibility of recurrence on the same side of the breast or chest wall, regional lymph nodes, or far-off organs; because MG has a limited field of view, the diagnosis of regional recurrences in MG is debated. Therefore, the US can be utilized as a complementary screening method. This has been investigated by Shin et al. [88]. Their study showed that axillary recurrence after BC and axillary treatment is rare in asymptomatic women with negative MG results. US screening of the whole breast after surgery does not assist in detecting axillary recurrence. Kim et al. [89] showed that complementary US had a lower interpretation rate of abnormalities and higher specificity (in women aged 50 years and older and in women two years after surgery) in women with a personal history of BC compared to women without a personal history of BC. Even though anti-hormonal treatment or aromatase inhibitors can decrease benign breast disease and false positive findings in the US [90], they did not affect the results of this study.

#### *Nanoparticles in US*

The low specificity of breast US for cancer detection is a classic problem that requires the use of a contrast agent [91]. Recent evidence suggests that NPs can be used for cancer detection and treatment as an US contrast agent. In an analysis of mesoporous silica NPs (MSNs) functionalized with the monoclonal antibody Herceptin<sup>®</sup>, Milgroom et al. [91] showed the potential of MSNs as a stable, biocompatible, and effective therapeutic and diagnostic (“theranostic”) agent for US-based breast cancer imaging, diagnosis, and treatment. Another study [92] has considered the usage of metal oxide NPs for cancer detection with US. In a major advance in 2021, Cao et al. [93] developed nanocarriers for sonodynamic therapy (SDT) of breast cancer.

#### **4. Magnetic Resonance Imaging (MRI)**

Magnetic resonance imaging has advantages such as its high sensitivity and specificity, and it is suitable for patients who have breast-conserving surgery. Its limitations include the high cost and time of scanning [94], false positive results, its limited use in patients with claustrophobia, and its hypersensitivity to contrast agents. Also, this method provides false positive results for extensive screening and the ideal BC stage [15]. According to the guidelines, MRI screening for high-risk populations is recommended, such as for women with BRCA mutations, women with Li-Fraumeni and other high-risk syndromes, women who received chest radiation between the ages of 10 and 30 years, and women with 20–25% or greater lifetime risk of developing breast cancer [95,96]. One of the critical issues with high-density breast imaging, particularly for small tumors, is reducing sensitivity below 40% [97]. However, magnetic resonance mammography (MRMG) has high sensitivity in diagnosing BC regardless of breast density [98]. The cost-effectiveness of MRMG compared to MG in patients with high breast density was evaluated by Kaiser et al. [99]. Their preliminary study showed that MRMG is a more accurate and less expensive modality than MG in patients with an intermediate risk of BC. They indicated that MR techniques such as parallel imaging and abbreviated protocols offer assistance in diminishing time and increase cost-effectiveness. According to their study, two-year screening with MRMG can be cost-effective for patients with DB tissue. In a study by Sippo et al. [100], the screening performance of breast MRI was evaluated. The authors’ research showed no difference in breast MR imaging screening performance for cancer detection rates among women with BRCA mutation or history of chest radiation therapy, women with a personal history of breast cancer, and women with a history of high-risk lesions. Women with a family history of breast cancer were found to have a lower cancer detection rate and positive predictive value compared to those with a BRCA mutation or previous chest radiation. Kim [101] conducted a retrospective study to compare abbreviated breast MRI with full-protocol MRI.

According to their investigation, abbreviated MRI has higher sensitivity and specificity than full-protocol MRI in women with an individual history of BC.

According to the obtained results, the sensitivity of breast MRI for breast carcinoma is between 88 and 100% in the diagnostic environment, and the characteristics of breast MRI reach 87% in the screening environment [102,103]. In other words, breast MRI is more sensitive than MG, US, or physical examination.

Vreemann et al.'s study [104] evaluated the complementary value of MG in women under and over 50 years of age and in BRCA mutation carriers. Their research shows that MG has restricted value when breast MRI is accessible. Still, it has an advantage over age 50 and in women without BRCA mutations who are more vulnerable to radiation-induced cancers. In another study, Gu et al. [105] examined molybdenum MG and MRI together to distinguish BC from benign tissue. The results of their research showed that MG with a molybdenum target is sensitive to calcification, but its detection rate by MRI is lower. On the other hand, MRI can show DB tumors well if MG is not appropriate for these patients. Hence, the authors showed that both methods increase sensitivity and diagnostic accuracy and decrease the hazard of non-diagnosis or misdiagnosis. In a study, the performance of breast MRI was compared with MG alone in women with a personal history of BC. The sensitivity of breast MRI in this study was different from previous studies. The authors stated that if cancer is detected on MG, multimodality breast imaging can lead to more false negative findings on breast MRI [106].

There have been studies comparing MRI with other breast imaging modalities, reported in a meta-analysis by Xiang et al. [107], in which 13 studies comparing CEM and MRI were reviewed. The study showed that the diagnostic sensitivity of the two methods is high, but their diagnostic specificity is relatively low. According to the authors' research, CEM and MRI are both effective methods for BC diagnosis, but the diagnostic performance of CEM is more effective than that of MRI. However, it has been determined that CEM has a smaller FOV than MRI, so it is less valuable for identifying chest wall invasion, internal breast metastasis, and axillary lymph node disease in patients with known BC [108]. Recently, the authors performed novel MRI modalities for a breast cancer diagnosis study, and they have reported that DTI, DWI, and DCE-MRI parameters can help diagnose breast cancer in the early stages [109]. In another study, Comstock et al. [103] compared abbreviated breast MRI and DBT to diagnose invasive BC in women with DB. These two methods were taken into consideration because DBT can increase the sensitivity and specificity of MG, and abbreviated MRI can reduce the complexity and cost of MRI. The study showed that abbreviated breast MRI has a higher BC detection rate than DBT. Another study [110] investigated MG, MRI, and US modalities as breast cancer screening methods. According to the authors' research, MRMG is a cost-effective technique for women with a high risk of breast cancer, but US is not; in other words, they showed that MRMG is more cost-effective than MG plus US.

In the study of Monika Graeser et al. [111], the ability of US and MRI to determine residual tumor size was investigated. The results of the study showed that in hormone receptor (HR)+/human epidermal growth factor receptor 2(HER2)+ and HR+/-HER2 breast cancer, MRI is less prone to underestimation than ultrasound, and ultrasound is associated with a lower risk of overestimating the size of the tumor.

Recently, positron emission tomography/magnetic resonance imaging (PET/MRI) has been considered a promising imaging method for breast cancer evaluation. Cancer is a very heterogeneous disease, and moreover, each patient is unique in terms of disease behavior and prognosis. Therefore, imaging methods that provide morphological data as well as functional data are very valuable. In the study of Valeria Romeo et al. [112], the role of PET/MRI in the evaluation of breast cancer was investigated. In this study, technical aspects of hybrid PET/MRI, new developments in MRI and PET, descriptions of new PET detectors, and clinical applications of hybrid PET/MRI of the breast are described. In this study, it is stated that despite the high costs and limited availability of PET/MRI, this imaging method is useful for morphological and functional assessment of breast cancer.

Furthermore, in a study by Janna Morawitz et al. [113], the results of CT, MRI, and [ $^{18}\text{F}$ ]-fluorodeoxyglucose positron emission tomography ([ $^{18}\text{F}$ ]-FDG PET/MRI) in determining the correct status of nodes in axillary (level I–III), supraclavicular, and internal mammary lymph nodes in patients with newly diagnosed breast cancer were compared. The results of this study showed that PET/MRI performs better in diagnosing lymph node metastasis, with higher speed and accuracy in all lymph node stations than CT or MRI. It has the highest sensitivity, and CT has the lowest sensitivity.

#### 4.1. Dynamic Contrast-Enhanced MRI

The DCE-MRI technique is a non-invasive and three-dimensional imaging technique that can show tumor angiogenesis and lymph node metastasis in BC [114]. Unlike MG, this technique is not limited by breast tissue density, but the main limitation is its non-specificity [115]. Other disadvantages are its long imaging time, high cost, high false positive rates, poor patient tolerance, contraindications such as a pacemaker or claustrophobia, the worry of gadolinium deposition in the brain [116–118], and the overlap between morphological features and kinetic patterns of benign and malignant lesions [119]. Also, the menstrual cycle can lead to a non-specific increase in breast parenchyma in DCE-MRI and, thus, false positives. Therefore, it is better to perform DCE-MRI between days 7 and 13 of the menstrual cycle [120]. In DCE-MRI, a pre-contrast  $T_1$ -weighted image is first taken, and then a sequence of  $T_1$ -weighted images after contrast is taken.

Although DCE-MRI has a high sensitivity for detecting BC, using gadolinium-based contrast agents is still a concern, so using non-contrast MR-based conductivity imaging has been considered. The result of Suh's et al. study [121] showed that the current performance of this method is lower compared to  $T_2$ WI, DWI, and MG. Still, conductivity imaging can reduce biopsy caused by DCE-MRI due to low conductivity values in benign lesions. In a study by Jochelson et al. [49], a comparison was made between bilateral CEM, conventional DM, and MRI in women with BC. The study showed that the DCE contrast agent persisted for at least 10 min after the infusion was complete, in contrast to the quick washout seen with MRI. In this manner, the arrangement in which the images are obtained is not essential. The authors demonstrated, moreover, that DCE could show lesions regardless of size; despite being sensitive to MR imaging, it presents fewer blunders.

In some studies, CEM and DCE-MRI were compared; for example, Maria Adele Marino et al. [122] conducted a retrospective study to compare the potential radiomic analysis of CEM and DCE-MRI of the breast for the non-invasive differentiation of invasive and non-invasive BC. Based on their conclusion, MR is costly and time-consuming and is contraindicated in cases such as claustrophobics and people with pacemakers or other implanted metallic materials. Therefore, they stated that CEM could replace MRI if MRI is unavailable or is contraindicated. In another study, Kamal et al. [123] compared these two methods. The authors found that DCE-MRI has advantages, such as fewer side effects of contrast agents and no ionizing radiation, which is better for examining inflammatory/malignant lesions. Broad breasts, deep-seated lesions, and lesions in hidden areas of MG should be identified. Though CEM is more accessible, shorter, and requires less training, it is better used for preoperative staging of breast cancer, post-treatment monitoring, and follow-up of patients receiving neoadjuvant chemotherapy. Also, in a study by Pötsch et al. [124], CEM and DCE-MRI were compared. The study showed that although CEM performs well for BC diagnosis, DCE-MRI has a higher sensitivity, and the ratio of negative probability to its pre-test probability is more elevated than CEM.

In other studies, DCE-MRI was compared with other breast imaging modalities. In a survey, Mann et al. [125] compared DCE-MRI, MG, and US. The authors stated that DCE-MRI is better than MG and US for the early detection of BC. They also noted that the complementary use of MG leads to an increase in BC diagnosis and a decrease in specificity. The complementary use of the US only causes a reduction in specificity, so it should not be used. The only disadvantage of MRI diagnosis is its high sensitivity for all types of BC, which can lead to overdiagnosis. Also, in a study [126], the sensitivity of MG with CE-MRI

was compared in women with different degrees of breast density. Based on the findings of this study, CE-MRI sensitivity is not affected by breast density due to the use of gadolinium. It is independent of breast density, whereas MG sensitivity decreases by approximately 20% with increasing breast density. In other words, the study showed that the sensitivity of CE-MRI in women with DB is higher than the sensitivity of MG.

In a study by Ramona Woitek et al. [127], the authors investigated the potential of hyperpolarized carbon-13 ( $^{13}\text{C}$ ) MRI and DCE in detecting early treatment response in breast cancer. The results of their study showed that after one cycle of neoadjuvant chemotherapy, a 34% decrease in the ratio of lactate to pyruvate labeled with  $^{13}\text{C}$  led to the correct identification of the patient, but DCE MRI showed an increase in the mean pharmacokinetic parameter transfer constant ( $K^{\text{trans}}$ ) (132%) and mean washout parameter ( $K_{\text{ep}}$ ) (31%). The results could be misinterpreted as a poor response to treatment. Therefore, the authors stated that  $^{13}\text{C}$  hyperpolarized MRI in combination with conventional multiparameter MRI improves response prediction.

#### 4.2. Diffusion-Weighted Imaging (DWI)

Although DCE-MRI is recommended for breast screening, this method is costly and time-consuming and requires the injection of a contrast agent. An abbreviated breast MRI can reduce time and cost, but a contrast agent still needs to be injected. Therefore, the potential of DW as a screening tool has been investigated [115]. The findings of this study showed that although DW is less sensitive than DCE MRI but higher than MG and US, it works better than MG and US and can be effective as a method for identifying malignancies hidden by MG. A study by Moy et al. [128] showed that DCE-MRI has been found to have a higher resolution in soft tissues than MRDW, and the positive predictive value of DCE-MRI is higher than the positive predictive value of MRI alone. Also, it is demonstrated that the sensitivity of DWI in diagnosing malignancy is higher compared to MRS and DCE, and it can also detect malignancy in all cases of indeterminate DCE [119].

It has been found that MRI often fails to distinguish between malignant and benign breast lesions. In contrast, DWI can identify breast lesions better than conventional MRI. The only significant issue related to DWI is finding the appropriate ADC value for diagnosing malignant and benign breast lesions. The value of the apparent diffusion coefficient (ADC) in normal tissue is higher than that in benign tissue, and in benign tissue, it is more heightened than in malignant tissue, so tissues can be diagnosed using MRDW and ADC measurement [129]. According to a meta-analysis study [130], the average ADC of benign breast lesions is more than  $1.00 \times 10^{-3} \text{ mm}^2/\text{s}$ , and most malignant lesions have ADC values less than  $2.0 \times 10^{-3} \text{ mm}^2/\text{s}$ . The authors of the study stated that  $1.00 \times 10^{-3} \text{ mm}^2/\text{s}$  could be used as a threshold value to distinguish malignant and benign breast lesions. The main limitation of DWI is that small cancer foci may not be seen on ADC maps [131].

In a study [132], the use of DWI as an independent parameter and multiparametric (mpMRI) using DCE-MRI and DWI for breast cancer diagnosis was investigated. Based on the authors' findings, DWI cannot be used as an independent and alternative parameter of DCE-MRI, because its spatial resolution is still very low. mpMRI has high sensitivity and specificity in diagnosis. The authors also showed that DCE-MRI is the most sensitive method for breast cancer diagnosis. Research has shown that DWI with a reduced field of view can create images with better quality and higher resolution than typical bilateral DWI, and this can also be used instead of DCE-MRI [133]. It should be noted that bilateral DWI has disadvantages such as magnetic susceptibility, chemical shifts, low signal-to-noise ratio, and low resolution [134].

#### 4.3. Magnetic Resonance Spectroscopy

In MRS, increased choline-containing compounds (the peak of Choline is 3.23 ppm [135]) in malignant breast lesions differentiate these from benign lesions and increase MRI specificity [136]. A study investigated in vivo  $^1\text{H}$ -MRS to distinguish malignant from benign breast lesions using the high choline (Cho) peak. Based on the findings of this study, the

choline peak has a suitable sensitivity and specificity for detecting malignant breast lesions. This study showed that malignant tumors with a Cho-positive peak were significantly larger than Cho-negative tumors. It was also stated that the sensitivity and specificity of the Cho peak are considerably lower than the multi-parametric MRMG, but placing the spectra located in the tissue around the tumor and the analysis of lipid peaks can increase this [137].

In some studies, MRS was compared with mpMRI. For example, in a retrospective study by Uma Sharma, multi-parametric MR combining DCE-MRI, DWI, and MRS data was evaluated to increase the sensitivity of breast lesion detection. The authors' research showed that mpMRI could improve the detection of breast malignancies, and the approaches could complement each other. They also showed that the sensitivity to detect malignancy was the highest for DWI compared to MRS and DCE-MRI [119]. In another study by Sodano et al. [138], the use of MRS for suspicious lesions in mpMRI was investigated. The study showed that the quantitative assessment of tCho from  $^1\text{H}$ -MRS can diagnose malignancy in breast lesions that are considered suspect by evaluating mp breast MRI using DCE,  $T_2W$ , and diffusion-weighted images. They also stated that a low concentration of tCho indicates the absence of metastasis to the lymph nodes.

#### 4.4. Magnetic Resonance Elastography

The MRE imaging technique is a non-invasive method used to measure tissues' stiffness or elasticity. This method uses sound waves in the range of 100 to 1000 Hz, and the imaging is performed using motion-sensitive MRI sequences. Breast MRE is a cross-sectional imaging method that quantifies the viscoelastic properties of breast tissues [139,140]. Due to the increased number of cells, collagen, and proteoglycans, BC has a higher stiffness than the surrounding normal tissues and benign lesions [140]. Manual touch lacks specificity and sensitivity, and MRE can overcome this limitation [141]. The most critical limit of MRE in BC is low spatial resolution and the detection of small focal lesions [142].

Today, MRE of the breast is in the research stage, and efforts are being made to reduce the scanning time and improve the spatial resolution. Also, the use of MRE to evaluate breast cancer and its ability to be used as a marker in malignant lesions needs more studies [141].

#### 4.5. $T_2$ and $T_2^*$ Mapping

$T_2$  and  $T_2^*$  relaxation time values are intrinsic properties of tissues. A considerable amount of literature has been published on the  $T_2$  and  $T_2^*$  relaxation time values of different tissues. These studies showed that tumors have significantly different  $T_2$  relaxation time values compared with normal tissues. Recent developments in MRI have led to a voxel-wise color map display of  $T_2$  and  $T_2^*$  relaxation time values of certain tissues as  $T_2$  and  $T_2^*$  map MRI sequences.  $T_2$  and  $T_2^*$  mapping is typically performed using a series of breath-hold spine-echo (SE) and gradient-echo (GRE) images at progressively increasing echo times (TE). For each pixel, the signal intensity curve is fitted to a simple exponential, resulting in an estimate of pixel  $T_2$  and  $T_2^*$  relaxation time and  $T_2$  and  $T_2^*$  map reconstruction. The  $T_2$  and  $T_2^*$  map provides a more objective detection and evaluation than standard anatomical images such as  $T_2$ -weighted and STIR images, which may be limited by susceptibilities or slow-motion artifacts and have a limited quantitative evaluation.

In a major advance, Liu et al. [143] studied the lesion  $T_2$  relaxation time change in breast cancer in response to neoadjuvant chemotherapy (NAC). The authors demonstrated that the lesion  $T_2$  relaxation time was reduced in response to the NAC. It has been suggested that  $T_2$  mapping is a potentially useful MRI protocol to assess the response of breast cancer tumors to NAC. In [144], the authors investigated  $T_2^*$  relaxation time in breast cancer and the association between lesion  $T_2^*$  values and pathological, clinical, and imaging data. They showed that the  $T_2^*$  relaxation time is significantly higher in invasive breast cancer than in ductal carcinoma. These results demonstrate that  $T_2^*$  mapping seems to be a useful

approach in the characterization and classification of breast cancer. Previous research [145] has indicated the classification of breast cancer as malignant and benign with lesion  $T_2$  relaxation time, with an area under the curve (AUC), sensitivity, and specificity of 0.731, 0.857, and 0.587, respectively.

In their groundbreaking paper, Meng et al. [146] used a novel quantitative MRI method, the synthetic MRI (syMRI), for breast cancer classification. The term syMRI has been used by Meng et al. [146] to refer to simultaneous  $T_1$  and  $T_2$  map generation and reconstruction (Figure 5) in one MRI scan within a few minutes and without requiring a gadolinium contrast agent injection. The authors point out that breast cancer has significantly higher  $T_1$  relaxation time and lower  $T_2$  relaxation time than benign breast lesions. Further analysis by Meng et al. [146] showed that the combination of  $T_1$  map and  $T_2$  map data for benign and malignant breast lesion classification could increase the AUC, sensitivity, and specificity to 0.978, 0.958, and 0.931, respectively.

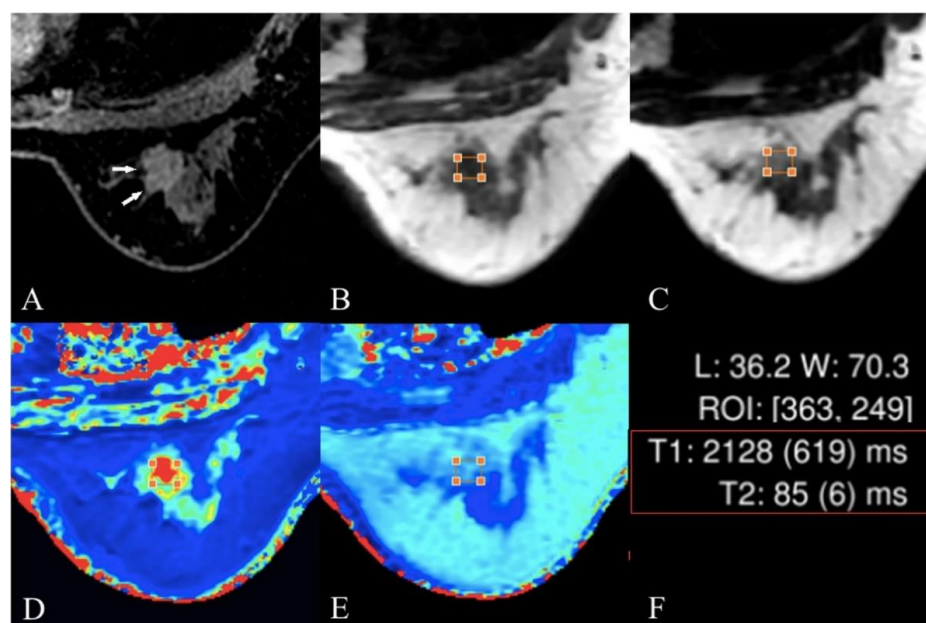


**Figure 5.** A 42-year-old female with malignant breast lesion. (A) Enhanced lesion is shown using white arrows in the image; (B)  $T_1$ -weighted images; (C)  $T_2$ -weighted images; (D)  $T_1$  map; (E)  $T_2$  map. The  $T_1$  and  $T_2$  values are shown in (F) [147]. “Reprinted with permission from Ref. [146]. 2020”. More details on “Copyright and Licensing” are available via the following link: <https://cancerimagingjournal.biomedcentral.com/articles/10.1186/s40644-020-00365-4> (accessed on 1 December 2023).

#### 4.6. Nanoparticles in MRI

In their review of recent inorganic NPs for breast cancer detection, Núñez et al. [148] identified different characteristics and benefits of superparamagnetic quantum dots and gold NPs in MRI imaging. Much work on the potential of iron oxide NPs as  $T_2$ -weighted contrast agents has been carried out. In her investigation into using fourth-generation dendrimer-coated iron oxide NPs ( $G_4@IONPs$ ) for cancer detection with MRI and treatment with hyperthermia, Salimi et al. [147] showed that  $G_4@IONPs$  significantly improved transverse relaxivity ( $r_2$ ), and they can be used as a  $T_2$ -weighted contrast agent. A review of the literature on using iron-oxide NPs in MRI [149] found that with a change in their structures, these NPs can also be used as a  $T_1$ -weighted MRI contrast agent. In a study that set out to determine the characteristics of poly(ethylene glycol) (PEG)-coated, manganese-doped iron oxide nanocomposites ( $Mn-IONPs@PEG$ ), Xiao et al. [150] found that  $Mn-IONPs@PEG$  have good transverse and longitudinal relaxivity properties, and they are a reasonable candidate for  $T_1/T_2$  dual-contrast MRI. Huang et al. [151] conclude that

ultrasmall MnO nanoparticles that are PEGylated via catechol-Mn chelation and conjugated with cRGD have a great potential for use as a  $T_1$ -weighted MRI contrast agent for the diagnosis of tumors. Surveys such as that conducted by Yao-Jiang Ye et al. [152] have shown that hybrid NPs co-loaded with copper sulfide (CuS) NPs and glucose oxidase (GOD) (CuS@GOD NPs) have in vivo feasibility for use in multiparametric MRI, including intravoxel incoherent motion diffusion-weighted imaging (IVIM-DWI) and  $R_2^*$  mapping for cancer detection and treatment response. It has been demonstrated that [153]  $Fe_3O_4$ @PD NPs result in  $T_1$  MRI darkening and brightening contrast enhancement at tumor sites, and the relative signal-to-noise ratio of the tumor can be used for distinguishing normal and tumor tissues.

## 5. Discussion

Different modalities used for breast imaging have successes and limitations. These have been evaluated by various researchers. The results showed that MG's sensitivity decreases with increasing breast density [10]. A comparison of results between FFDM and DBT has demonstrated the following: An overlap of breast tissue in FFDM can be reduced with DBT [24]. Unlike FFDM, DBT can visualize the margin of the lesion [31]. DBT with SM is a better method than FFDM for detecting mass, calcification, and asymmetry [36]. DBT can detect more cancers than DM in all age and density groups. False positive findings due to asymmetric density are lower except in very dense breasts [28]. The results of a study showed that adding DBT to FFDM can lead to increased sensitivity, specificity, and positive predictive value, decreased false positive rate, increased cancer detection rate, and increased sensitivity and specificity. Though using SM instead of DM in combination with DBT causes a slight change in sensitivity or specificity, it can be concluded that SM can be a good substitute for DM when using DBT [40].

From the point of view of comparison among different modalities for BC diagnosis, the summary of results is illustrated in Table 1, and they have different criteria as follows: EM and DM showed that CEM has higher sensitivity and specificity than DM [49,51]. Its comparison with MG has shown that CEM is more sensitive than MG for detecting BC, and it has higher diagnostic accuracy than MG alone and MG combined with US [62]. Still, CEM has less specificity than MG [53]. Another study has shown that CEM has a higher sensitivity than DBT, but the description of the margin and exact location of breast lesions is better evaluated in DBT [54]. Another comparison has shown that CEM has a detection rate similar to US and MRI and significantly higher than FFDM [57]. CEM is more accurate than DM and DBT and is comparable to DCE-MRI in evaluating breast malignancy [58]. A comparison between CEM and US showed that axillary lesions and lymph nodes might not be seen on CEM, but the US can show abnormalities in these areas [81]. Also, it showed that the ability of the US to detect benign lesions is higher than CEM [82]. Ultrasound imaging is better than MG for detecting dense breasts, because dense tissue and breast cancer are seen as white in MG, whereas dense tissue is echogenic in US, and BC is hypogenic [84]. The magnetic resonance imaging method has higher sensitivity than MG, US, or physical examination and is more cost-effective than MG plus US [110]. A comparison of CEM and MRI has shown that CEM is less valuable than MRI for detecting chest wall invasion, internal breast metastasis, and axillary lymph node disease in patients with known BC due to its smaller FOV [108]. One of the advantages of DCE-MRI is that unlike MG, it is not limited by breast tissue density [126], but the main limitation is its non-specificity [115]. Another is that the menstrual cycle can lead to a non-specific increase in breast parenchyma in DCE, resulting in false positives. Therefore, it is better to perform DCE between days 7 and 13 of the menstrual cycle [120]. Findings show that DCE-MRI is suitable for investigating inflammatory/malignant lesions, broad breasts, deep lesions, and lesions in hidden areas of MG compared with CEM. On the other hand, CEM is better for preoperative staging of breast cancer, post-operative monitoring, treatment, and follow-up of patients receiving neoadjuvant chemotherapy [123]. Also, DCE-MRI is better than MG and US for early detection of BC, and its sensitivity is independent of breast

density and higher than MG [126]. Indeed, a comparison was made between DW and other imaging modalities, showing that although DW is less sensitive than DCE MRI, it performs better than MG and US and can be effective as a method for identifying hidden MG malignancies [115]. It has also been shown that the sensitivity of DWI in diagnosing malignancy is higher compared to MRS and DCE, and it can detect malignancy in all cases of indeterminate DCE [119]. The only significant issue related to DWI is finding the appropriate ADC value;  $1.00 \times 10^{-3} \text{ mm}^2/\text{s}$  can be used as a threshold value to distinguish between malignant and benign breast lesions [130]. It has been reported that the sensitivity and specificity of the Cho peak in MRS are significantly lower than that of multi-parameter MRMG. Still, including spectra located in the peri-tumor tissue and the analysis of lipid peaks can increase sensitivity and specificity [137]. Moreover, an imaging modality that is still in the research stage is MRE. MRE can overcome the limitations of manual touch, such as the lack of specificity and sensitivity [142], and due to the increase in the number of cells, collagen, and proteoglycans in BC compared to surrounding normal tissues and benign lesions, MRE can distinguish areas of BC due to their higher stiffness [141].

**Table 1.** Summary of successes and limitations in recent studies of breast diagnosis modalities.

Modality	Advantages	Disadvantages	Diagnostic Performance			Diagnostic Performance for:	Ref.
			AUC	Sensitivity	Specificity		
MG	<ul style="list-style-type: none"> <li>- Detects BC, benign tumors, and cysts</li> <li>- Finds mammary gland calcification</li> </ul>	<ul style="list-style-type: none"> <li>- Not suitable for people under 40 years</li> <li>- Cannot be undertaken more than twice a year</li> <li>- Limited in imaging DB tissue</li> </ul>	N/A	97%	64.5%	Breast cancer detection	[14–16]
DBT	<ul style="list-style-type: none"> <li>- An increase in cancer detection and a decrease in the recall rate compared to MG</li> <li>- Better characterizes invasive lobular carcinoma, lower histologic-grade HER-2-negative lesions, lesions presenting as masses, or lesions with architectural distortion compared to FFDM</li> <li>- Visualizes the lesion margin better than FFDM</li> <li>- DBT with SM is a better method than FFDM for detecting mass, calcification, and asymmetry</li> </ul>	<ul style="list-style-type: none"> <li>- Limited in imaging DB tissue</li> </ul>	N/A	95.5%	78.8%	Malignancy detection	[27,30,31,35]
CEM	<ul style="list-style-type: none"> <li>- Higher sensitivity and specificity than MG and DM alone</li> <li>- Has sensitivity and specificity comparable to CE-MRI</li> <li>- Has sensitivity higher than SM, DBT, and DBT plus US</li> <li>- Has a detection rate similar to US and MRI and significantly higher than FFDM</li> <li>- Has a high sensitivity in preoperative staging of BC compared to DM</li> </ul>	<ul style="list-style-type: none"> <li>- Has less specificity than MG</li> <li>- Visualizes the lesion margin less compared to DBT</li> <li>- Not suitable in patients with spreading of unifocal disease, ductal carcinoma in situ histotypes, lesion size less than 10 mm, and index lesion with microcalcification</li> <li>- Need to inject contrast agents</li> <li>- CEM-guided biopsy is unavailable</li> <li>- Does not have sufficient sensitivity to detect poorly advanced cancers</li> <li>- Does not show cancers with increased parenchyma in the background or near the chest wall</li> </ul>	(0.768–0.924)	(86.2–98%)	(57.9–94.1%)	Cancer detection and breast cancer classification into malignant and benign	[49,51,53,54,57,62–64]



Table 1. Cont.

Modality	Advantages	Disadvantages	Diagnostic Performance			Diagnostic Performance for:	Ref.
			AUC	Sensitivity	Specificity		
US	<ul style="list-style-type: none"> <li>- Does not require ionizing radiation or intravenous contrast</li> <li>- Portability, lower cost than MG, the perfect imaging tool for biopsy, and versatility, as it distinguishes cystic masses from solid masses</li> <li>- Can be utilized as an early diagnosis tool</li> <li>- Shows axillary and lymph node lesions that might not be seen in CEM</li> <li>- Detect benign lesions is higher than that of CEM</li> <li>- Can distinguish dense tissue from breast cancer, unlike MG</li> </ul>	<ul style="list-style-type: none"> <li>- Depends on the experience of the radiologist</li> <li>- Has unsatisfactory false positives and false negatives in asymptomatic women</li> </ul>	N/A	(49–90.6%)	(34–88.4%)	Screening of dense breast and breast cancer classification into the malignant and benign	[76,81,82, 84–86]
MRI	<ul style="list-style-type: none"> <li>- High sensitivity and specificity; suitable for patients who have breast-conserving surgery</li> <li>- High sensitivity in diagnosing BC regardless of breast density</li> <li>- Breast MRI is more sensitive than MG, US, or physical examination</li> <li>- More valuable for identifying chest wall invasion, internal breast metastasis, and axillary lymph node than CEM</li> <li>- Abbreviated breast MRI has a higher BC detection rate than DBT</li> <li>- MRMG is more cost-effective than MG plus US</li> </ul>	<ul style="list-style-type: none"> <li>- High cost and time required for scanning</li> <li>- False positive results, not suitable in patients with claustrophobia</li> <li>- Not suitable for hypersensitivity to contrast agent</li> </ul>	0.93	(51–100%)	(94.9–96.1%)	Breast cancer detection	[15,94,98, 102,103, 108,109, 122]
DCE-MRI	<ul style="list-style-type: none"> <li>- Not limited by breast tissue density, unlike MG</li> <li>- Can show lesions regardless of size</li> <li>- Has fewer side effects of contrast agents and no ionizing radiation vs. CEM</li> <li>- Has a higher sensitivity than CEM</li> <li>- DCE-MRI is better than MG and US for the early detection of BC</li> </ul>	<ul style="list-style-type: none"> <li>- Non-specificity</li> <li>- Time-consuming</li> <li>- Costly</li> <li>- High false positive rates</li> <li>- Poor patient tolerance</li> <li>- Has contraindications</li> <li>- Requires the injection of a contrast agent</li> <li>- Overlap between morphological features and kinetic patterns of benign and malignant lesions</li> <li>- Menstrual cycle can lead to a non-specific increase in breast parenchyma</li> </ul>	N/A	(81–100%)	~97%	Breast cancer detection	[49,115–120,123–125]
DWI	<ul style="list-style-type: none"> <li>- Works better than MG and US</li> <li>- Highest sensitivity of detection compared to DCE-MRI and MRS</li> <li>- Can identify breast lesions better than conventional MRI</li> </ul>	<ul style="list-style-type: none"> <li>- Less sensitive than DCE MRI but more sensitive than MG and US</li> <li>- Less resolution in soft tissues than DCE MRI</li> <li>- Spatial resolution is still very low</li> <li>- Small cancer foci may not be seen on ADC maps</li> </ul>	0.85	(63–100%)	(46–97%)	Breast cancer classification into malignant and benign	[115,119, 128,129, 131,132]

Abbreviations: AUC: area under the curve; Ref: references; MG: mammography; DBT: digital breast tomosynthesis; CEM: contrast-enhanced mammography; US: ultrasound imaging; MRI: magnetic resonance imaging; DCE-MRI: dynamic contrast-enhanced MRI; DWI: diffusion-weighted imaging.

The review of literature indicates that researchers have used NPs for breast cancer detection with different imaging modalities, and a strong relationship between image contrast, SNR, etc. and using NPs has been reported. Table 2 presents an overview of some NPs and their application in breast cancer detection with different imaging modalities. MRI is a major area of interest within the field of using NPs for breast cancer detection. Fe, Cu, and Mn NPs are some of the most widely used NPs for breast cancer detection by MRI with

T<sub>1</sub>, T<sub>2</sub>, and DWI image weights. Overall, the use of nanoparticles for breast cancer detection offers several advantages over contrast agents such as iodine and gadolinium, including improved contrast, targeted delivery, better imaging, longer retention time, and reduced toxicity. Nanoparticles can produce a much stronger signal compared to conventional contrast agents, which makes them better at enhancing contrast and improving the accuracy of breast cancer detection. Nanoparticles can be designed to target cancer cells specifically, which means they can be used to deliver drugs or other therapies directly to the cancer cells, reducing the risk of side effects and improving treatment efficacy [154]. Nanoparticles can be engineered to emit light or magnetic signals, which can be detected using specialized imaging techniques such as MRI and optical imaging [155]. This allows for better imaging of breast tissue and more accurate detection of cancer. Nanoparticles can remain in the body for longer periods of time compared to contrast agents, which means they can be used for longer imaging sessions and can provide more comprehensive information about the breast tissue [156,157]. Some contrast agents such as gadolinium have been associated with toxicity in certain patients, whereas nanoparticles are generally considered safer and less likely to cause adverse effects [156,158]. The major limitation of NP studies for cancer detection includes the studies' data, which are presented, as they are based on in vivo studies. Optical and photoacoustic imaging techniques are commonly employed in preclinical investigations. Optical and photoacoustic imaging are limited in their ability to penetrate deep into the breast tissue. The resolution of these methods is limited by the wavelength of the light used, which can make it difficult to distinguish between small tumors and healthy tissue and does not provide specific information about the molecular and cellular characteristics of tumors [159]. Further research might investigate the clinical use of NPs and preclinical imaging such as optical and photoacoustic imaging for human imaging.

**Table 2.** Summary of recent studies using nanoparticles for breast cancer detection.

Authors and Ref.	Nanoparticles	Imaging Modality	Application		Conclusion
			Imaging	Therapy	
Naha et al. [65]	Gold–silver alloy nanoparticles (GSAN)	DEM and CT	✓		GSAN produces strong DEM and CT contrast in images and has potential for breast cancer screening.
Nieves et al. [66]	Silver telluride NPs (Ag <sub>2</sub> Te NPs)	DEM and CT			Strong X-ray contrast for breast cancer screening.
Karunamuni et al. [67]	Silica-encapsulated silver NPs	DEM	✓		Silver nanoparticles produce strong contrast in vivo using DEM imaging systems for breast cancer detection.
Cole et al. [68]	Bisphosphonate-functionalized gold NPs (BP-Au NPs)	CT and X-ray imaging	✓		Targeted BP-Au NPs enabled improved sensitivity and specificity for the detection of microcalcifications in breast cancer with CT imaging.
Cole et al. [69]	Bisphosphonate-functionalized gold NPs (BP-Au NPs)	CT and X-ray imaging	✓		Improved sensitivity and specificity for microcalcification detection in radiographically dense mammary tissues.
Milgroom et al. [91]	Mesoporous silica nanoparticles (MSNs), functionalized with the monoclonal antibody Herceptin®	US	✓	✓	The results demonstrated that MSNs are a stable, biocompatible, and effective diagnostic and therapeutic agent for US breast cancer imaging, diagnosis, and treatment.
Cao et al. [93]	Exosome-based NPs	US		✓	Exosome-based NPs could serve as effective nanosensitizers for safe and targeted cancer treatment.

Table 2. Cont.

Authors and Ref.	Nanoparticles	Imaging Modality	Application		Conclusion
			Imaging	Therapy	
Salimi et al. [148]	Fourth-generation dendrimer-coated iron-oxide nanoparticles (G <sub>4</sub> @IONPs)	MRI	✓	✓	The results showed that G <sub>4</sub> @IONPs improved transverse relaxivity (r <sub>2</sub> ) significantly.
Xiao et al. [150]	Poly (ethylene glycol) (PEG)-coated, manganese-doped iron oxide nanocomposites (Mn-IONPs@PEG)	MRI	✓		The Mn-IONPs@PEG exhibited good properties for MRI imaging as a T <sub>1</sub> /T <sub>2</sub> dual-contrast MRI contrast agent for cancer detection.
Huang et al. [151]	PEGylated ultrasmall MnO NPs	MRI	✓		MnO NPs showed a great potential for the T <sub>1</sub> -weighted MRI diagnosis of tumors.
Tao et al. [153]	Small Fe <sub>3</sub> O <sub>4</sub> NPs	MRI	✓	✓	Fe <sub>3</sub> O <sub>4</sub> @PD-based system has the potential to be a multifunctional nanodrug delivery system and a smart theragnostic platform for cancer detection and treatment.

Abbreviations: CT: computed tomography, DEM: dual-energy mammography, NP: nanoparticles, US: ultrasound, MRI: magnetic resonance imaging.

## 6. Conclusions

Breast cancer imaging modalities are of great importance at early stages. Based on the literature, different imaging modalities have different abilities and successes in depicting the breast tissue. For instance, with DB, US and DCE-MRI are appropriate, whereas MG is inappropriate. It has been determined that the DCE-MRI technique is suitable for examining DBT tumor margins and axillary lesions. On the other hand, US is useful for examining lymph nodes, inflammatory/malignant lesions, broad breast, deep lesions, lesions in hidden areas of MG, and the stage before postoperative monitoring and treatment.

The evidence from this study suggests that using NPs for breast cancer detection with different imaging modalities, especially MRI, can increase the SNR and image contrast of breast images. This research extends our knowledge of using NPs for breast cancer detection with different imaging modalities. Therefore, considering the purpose of breast tissue imaging, the appropriate modality should be selected.

This review article could prove useful from a tutorial and educational point of view for all radiologists, medical students, and researchers who are interested in breast cancer diagnosis. The limitation of this article is that it may not have covered all recent findings in all parts of the world.

**Author Contributions:** Conceptualization, D.S.-G.; Methodology, D.S.-G., F.A., A.K. and S.S.-G.; Validation, D.S.-G., F.A. and A.K.; Investigation, D.S.-G., F.A., A.K. and S.S.-G.; Resources, D.S.-G.; Data Curation, D.S.-G., F.A., A.K. and S.S.-G.; Writing—Original Draft Preparation, F.A.; Writing—Review and Editing, D.S.-G. and A.K.; Supervision, D.S.-G.; Project Administration, D.S.-G.; Funding Acquisition, D.S.-G. All authors have read and agreed to the published version of the manuscript.

**Funding:** This study was funded by Isfahan University of Medical Sciences, Isfahan, Iran.

**Institutional Review Board Statement:** This article does not contain any studies with human participants or animals performed by any of the authors.

**Data Availability Statement:** The data presented in this study are available on request from the corresponding author.

**Conflicts of Interest:** The authors declare no conflict of interest.

## References

1. Singletary, S.E. Rating the risk factors for breast cancer. *Ann. Surg.* **2003**, *237*, 474–482. [[CrossRef](#)]
2. Le Boulc'h, M.; Bekhouche, A.; Kermarrec, E.; Milon, A.; Abdel Wahab, C.; Zilberman, S.; Chabbert-Buffet, N.; Thomassin-Naggara, I. Comparison of breast density assessment between human eye and automated software on digital and synthetic mammography: Impact on breast cancer risk. *Diagn. Interv. Imaging* **2020**, *101*, 811–819. [[CrossRef](#)]
3. Huang, J.; Chan, P.S.; Lok, V.; Chen, X.; Ding, H.; Jin, Y.; Yuan, J.; Lao, X.Q.; Zheng, Z.J.; Wong, M.C. Global incidence and mortality of breast cancer: A trend analysis. *Aging* **2021**, *13*, 5748–5803. [[CrossRef](#)]
4. Duggento, A.; Conti, A.; Mauriello, A.; Guerrisi, M.; Toschi, N. Deep computational pathology in breast cancer. *Semin. Cancer Biol.* **2021**, *72*, 226–237. [[CrossRef](#)]
5. Ding, K.; Zhou, M.; Wang, H.; Gevaert, O.; Metaxas, D.; Zhang, S. A large-scale synthetic pathological dataset for deep learning-enabled segmentation of breast cancer. *Sci. Data* **2023**, *10*, 231. [[CrossRef](#)]
6. Qu, H.; Zhou, M.; Yan, Z.; Wang, H.; Rustgi, V.K.; Zhang, S.; Gevaert, O.; Metaxas, D.N. Genetic mutation and biological pathway prediction based on whole slide images in breast carcinoma using deep learning. *NPJ Precis. Oncol.* **2021**, *5*, 87. [[CrossRef](#)]
7. Ibrahim, A.; Gamble, P.; Jaroensri, R.; Abdelsamea, M.M.; Mermel, C.H.; Chen, P.-H.C.; Rakha, E.A. Artificial intelligence in digital breast pathology: Techniques and applications. *Breast* **2020**, *49*, 267–273. [[CrossRef](#)]
8. Bhushan, A.; Gonsalves, A.; Menon, J.U. Current state of breast cancer diagnosis, treatment, and theranostics. *Pharmaceutics* **2021**, *13*, 723. [[CrossRef](#)]
9. Moy, L.; Heller, S.L.; Bailey, L.; D'Orsi, C.; DiFlorio, R.M.; Green, E.D.; Holbrook, A.I.; Lee, S.J.; Lourenco, A.P.; Mainiero, M.B.; et al. ACR Appropriateness Criteria<sup>®</sup> Palpable Breast Masses. *J. Am. Coll. Radiol.* **2017**, *14*, S203–S224. [[CrossRef](#)]
10. Nikolova, N.K. Microwave imaging for breast cancer. *IEEE Microw. Mag.* **2011**, *12*, 78–94. [[CrossRef](#)]
11. Løberg, M.; Lousdal, M.L.; Bretthauer, M.; Kalager, M. Benefits and harms of mammography screening. *Breast Cancer Res.* **2015**, *17*, 63. [[CrossRef](#)] [[PubMed](#)]
12. Dibden, A.; Offman, J.; Duffy, S.W.; Gabe, R. Worldwide review and meta-analysis of cohort studies measuring the effect of mammography screening programmes on incidence-based breast cancer mortality. *Cancers* **2020**, *12*, 976. [[CrossRef](#)] [[PubMed](#)]
13. Hendrick, R.E. Radiation Doses and Risks in Breast Screening. *J. Breast Imaging* **2020**, *2*, 188–200. [[CrossRef](#)]
14. Zeeshan, M.; Salam, B.; Khalid, Q.S.B.; Alam, S.; Sayani, R. Diagnostic accuracy of digital mammography in the detection of breast cancer. *Cureus* **2018**, *10*, e2448. [[CrossRef](#)] [[PubMed](#)]
15. He, Z.; Chen, Z.; Tan, M.; Elingarami, S.; Liu, Y.; Li, T.; Deng, Y.; He, N.; Li, S.; Fu, J. A review on methods for diagnosis of breast cancer cells and tissues. *Cell Prolif.* **2020**, *53*, e12822. [[CrossRef](#)] [[PubMed](#)]
16. Mandelorn, M.T.; Oestreicher, N.; Porter, P.L.; White, D.; Finder, C.A.; Taplin, S.H.; White, E. Breast density as a predictor of mammographic detection: Comparison of interval-and screen-detected cancers. *J. Natl. Cancer Inst.* **2000**, *92*, 1081–1087. [[CrossRef](#)] [[PubMed](#)]
17. Seeram, E. Full-Field Digital Mammography. In *Digital Radiography: Physical Principles and Quality Control*; Seeram, E., Ed.; Springer: Singapore, 2019; pp. 111–123. [[CrossRef](#)]
18. Song, S.Y.; Park, B.; Hong, S.; Kim, M.J.; Lee, E.H.; Jun, J.K. Comparison of Digital and Screen-Film Mammography for Breast-Cancer Screening: A Systematic Review and Meta-Analysis. *J. Breast Cancer* **2019**, *22*, 311–325. [[CrossRef](#)]
19. Farber, R.; Houssami, N.; Wortley, S.; Jacklyn, G.; Marinovich, M.L.; McGeehan, K.; Barratt, A.; Bell, K. Impact of Full-Field Digital Mammography Versus Film-Screen Mammography in Population Screening: A Meta-Analysis. *JNCI J. Natl. Cancer Inst.* **2020**, *113*, 16–26. [[CrossRef](#)]
20. Pisano, E.D.; Gatsonis, C.; Hendrick, E.; Yaffe, M.; Baum, J.K.; Acharyya, S.; Conant, E.F.; Fajardo, L.L.; Bassett, L.; D'Orsi, C.; et al. Diagnostic performance of digital versus film mammography for breast-cancer screening. *N. Engl. J. Med.* **2005**, *353*, 1773–1783. [[CrossRef](#)]
21. Posso, M.; Louro, J.; Sánchez, M.; Román, M.; Vidal, C.; Sala, M.; Baré, M.; Castells, X.; Group, B.S. Mammographic breast density: How it affects performance indicators in screening programmes? *Eur. J. Radiol.* **2019**, *110*, 81–87. [[CrossRef](#)]
22. Kerlikowske, K.; Hubbard, R.A.; Miglioretti, D.L.; Geller, B.M.; Yankaskas, B.C.; Lehman, C.D.; Taplin, S.H.; Sickles, E.A.; Consortium, B.C.S. Comparative effectiveness of digital versus film-screen mammography in community practice in the United States: A cohort study. *Ann. Intern. Med.* **2011**, *155*, 493–502. [[CrossRef](#)] [[PubMed](#)]
23. Korhonen, K.E.; Weinstein, S.P.; McDonald, E.S.; Conant, E.F. Strategies to increase cancer detection: Review of true-positive and false-negative results at digital breast tomosynthesis screening. *Radiographics* **2016**, *36*, 1954. [[CrossRef](#)] [[PubMed](#)]
24. Baker, J.A.; Lo, J.Y. Breast tomosynthesis: State-of-the-art and review of the literature. *Acad. Radiol.* **2011**, *18*, 1298–1310. [[CrossRef](#)] [[PubMed](#)]
25. Gennaro, G.; Bernardi, D.; Houssami, N. Radiation dose with digital breast tomosynthesis compared to digital mammography: Per-view analysis. *Eur. Radiol.* **2018**, *28*, 573–581. [[CrossRef](#)] [[PubMed](#)]
26. Georgian-Smith, D.; Obuchowski, N.A.; Lo, J.Y.; Brem, R.F.; Baker, J.A.; Fisher, P.R.; Rim, A.; Zhao, W.; Fajardo, L.L.; Mertelmeier, T. Can Digital Breast Tomosynthesis Replace Full-Field Digital Mammography? A Multireader, Multicase Study of Wide-Angle Tomosynthesis. *Am. J. Roentgenol.* **2019**, *212*, 1393–1399. [[CrossRef](#)] [[PubMed](#)]
27. Ali, E.A.; Adel, L. Study of role of digital breast tomosynthesis over digital mammography in the assessment of BIRADS 3 breast lesions. *Egypt. J. Radiol. Nucl. Med.* **2019**, *50*, 48. [[CrossRef](#)]

28. Østerås, B.H.; Martinsen, A.C.T.; Gullien, R.; Skaane, P. Digital Mammography versus Breast Tomosynthesis: Impact of Breast Density on Diagnostic Performance in Population-based Screening. *Radiology* **2019**, *293*, 60–68. [[CrossRef](#)]
29. Dang, P.A.; Wang, A.; Senapati, G.M.; Ip, I.K.; Lacson, R.; Khorasani, R.; Giess, C.S. Comparing Tumor Characteristics and Rates of Breast Cancers Detected by Screening Digital Breast Tomosynthesis and Full-Field Digital Mammography. *Am. J. Roentgenol.* **2019**, *214*, 701–706. [[CrossRef](#)]
30. Lee, S.H.; Jang, M.J.; Kim, S.M.; Yun, B.L.; Rim, J.; Chang, J.M.; Kim, B.; Choi, H.Y. Factors affecting breast cancer detectability on digital breast tomosynthesis and two-dimensional digital mammography in patients with dense breasts. *Korean J. Radiol.* **2019**, *20*, 58–68. [[CrossRef](#)]
31. Romanucci, G.; Mercogliano, S.; Carucci, E.; Cina, A.; Zantedeschi, E.; Caneva, A.; Benassuti, C.; Fornasa, F. Diagnostic accuracy of resection margin in specimen radiography: Digital breast tomosynthesis versus full-field digital mammography. *La Radiol. Medica* **2021**, *126*, 768–773. [[CrossRef](#)]
32. Heindel, W.; Weigel, S.; Gerß, J.; Hense, H.-W.; Sommer, A.; Krischke, M.; Kerschke, L. Digital breast tomosynthesis plus synthesised mammography versus digital screening mammography for the detection of invasive breast cancer (TOSYMA): A multicentre, open-label, randomised, controlled, superiority trial. *Lancet Oncol.* **2022**, *23*, 601–611. [[CrossRef](#)] [[PubMed](#)]
33. You, C.; Zhang, Y.; Gu, Y.; Xiao, Q.; Liu, G.; Shen, X.; Yang, W.; Peng, W. Comparison of the diagnostic performance of synthesized two-dimensional mammography and full-field digital mammography alone or in combination with digital breast tomosynthesis. *Breast Cancer* **2020**, *27*, 47–53. [[CrossRef](#)] [[PubMed](#)]
34. Choi, J.S.; Han, B.-K.; Ko, E.Y.; Kim, G.R.; Ko, E.S.; Park, K.W. Comparison of synthetic and digital mammography with digital breast tomosynthesis or alone for the detection and classification of microcalcifications. *Eur. Radiol.* **2019**, *29*, 319–329. [[CrossRef](#)] [[PubMed](#)]
35. Choi, Y.; Woo, O.-h.; Shin, H.-s.; Cho, K.R.; Seo, B.K.; Choi, G.-Y. Quantitative analysis of radiation dosage and image quality by digital breast tomosynthesis (DBT) with two-dimensional synthetic mammography and full-field digital mammography (FFDM). *Clin. Imaging* **2019**, *55*, 12–17. [[CrossRef](#)] [[PubMed](#)]
36. Falomo, E.; Myers, K.; Reichel, K.F.; Carson, K.A.; Mullen, L.; Di Carlo, P.; Harvey, S. Impact of insurance coverage and socioeconomic factors on screening mammography patients' selection of digital breast tomosynthesis versus full-field digital mammography. *Breast J.* **2018**, *24*, 1091–1093. [[CrossRef](#)] [[PubMed](#)]
37. Barca, P.; Lamastra, R.; Aringhieri, G.; Tucciariello, R.M.; Traino, A.; Fantacci, M.E. Comprehensive assessment of image quality in synthetic and digital mammography: A quantitative comparison. *Australas. Phys. Eng. Sci. Med.* **2019**, *42*, 1141–1152. [[CrossRef](#)] [[PubMed](#)]
38. Murakami, R.; Uchiyama, N.; Tani, H.; Yoshida, T.; Kumita, S. Comparative analysis between synthetic mammography reconstructed from digital breast tomosynthesis and full-field digital mammography for breast cancer detection and visibility. *Eur. J. Radiol. Open* **2020**, *7*, 100207. [[CrossRef](#)] [[PubMed](#)]
39. Singla, D.; Chaturvedi, A.K.; Aggarwal, A.; Rao, S.A.; Hazarika, D.; Mahawar, V. Comparing the diagnostic efficacy of full field digital mammography with digital breast tomosynthesis using BIRADS score in a tertiary cancer care hospital. *Indian J. Radiol. Imaging* **2018**, *28*, 115–122. [[CrossRef](#)]
40. Skaane, P.; Bandos, A.I.; Niklason, L.T.; Sebuødegård, S.; Østerås, B.H.; Gullien, R.; Gur, D.; Hofvind, S. Digital mammography versus digital mammography plus tomosynthesis in breast cancer screening: The Oslo Tomosynthesis Screening Trial. *Radiology* **2019**, *291*, 23–30. [[CrossRef](#)]
41. Yi, A.; Chang, J.M.; Shin, S.U.; Chu, A.J.; Cho, N.; Noh, D.-Y.; Moon, W.K. Detection of noncalcified breast cancer in patients with extremely dense breasts using digital breast tomosynthesis compared with full-field digital mammography. *Br. J. Radiol.* **2019**, *92*, 20180101. [[CrossRef](#)]
42. Alabousi, M.; Wadera, A.; Kashif Al-Ghita, M.; Kashef Al-Ghetaa, R.; Salameh, J.P.; Pozdnyakov, A.; Zha, N.; Samoilov, L.; Dehmoobad Sharifabadi, A.; Sadeghirad, B.; et al. Performance of Digital Breast Tomosynthesis, Synthetic Mammography, and Digital Mammography in Breast Cancer Screening: A Systematic Review and Meta-Analysis. *J. Natl. Cancer Inst.* **2021**, *113*, 680–690. [[CrossRef](#)] [[PubMed](#)]
43. Khanani, S.; Hruska, C.; Lazar, A.; Hoernig, M.; Hebecker, A.; Obuchowski, N. Performance of Wide-Angle Tomosynthesis with Synthetic Mammography in Comparison to Full Field Digital Mammography. *Acad. Radiol.* **2022**, *30*, 3–13. [[CrossRef](#)] [[PubMed](#)]
44. Zuckerman, S.P.; Conant, E.F.; Keller, B.M.; Maidment, A.D.; Barufaldi, B.; Weinstein, S.P.; Synnestvedt, M.; McDonald, E.S. Implementation of synthesized two-dimensional mammography in a population-based digital breast tomosynthesis screening program. *Radiology* **2016**, *281*, 730. [[CrossRef](#)] [[PubMed](#)]
45. Bernardi, D.; Macaskill, P.; Pellegrini, M.; Valentini, M.; Fantò, C.; Ostillio, L.; Tuttobene, P.; Luparia, A.; Houssami, N. Breast cancer screening with tomosynthesis (3D mammography) with acquired or synthetic 2D mammography compared with 2D mammography alone (STORM-2): A population-based prospective study. *Lancet Oncol.* **2016**, *17*, 1105–1113. [[CrossRef](#)] [[PubMed](#)]
46. Tamam, N.; Salah, H.; Rabbaa, M.; Abuljoud, M.; Sulieman, A.; Alkhorayef, M.; Bradley, D.A. Evaluation of patients radiation dose during mammography imaging procedure. *Radiat. Phys. Chem.* **2021**, *188*, 109680. [[CrossRef](#)]
47. Ghaderi, K.F.; Phillips, J.; Perry, H.; Lotfi, P.; Mehta, T.S. Contrast-enhanced mammography: Current applications and future directions. *Radiographics* **2019**, *39*, 1907–1920. [[CrossRef](#)] [[PubMed](#)]
48. Diekmann, F.; Lawaczeck, R. Contrast Media in CEDM. In *Contrast-Enhanced Digital Mammography (CEDM)*; Nori, J., Kaur, M., Eds.; Springer International Publishing: Cham, Switzerland, 2018; pp. 25–33. [[CrossRef](#)]

49. Jochelson, M.S.; Dershaw, D.D.; Sung, J.S.; Heerdt, A.S.; Thornton, C.; Moskowitz, C.S.; Ferrara, J.; Morris, E.A. Bilateral contrast-enhanced dual-energy digital mammography: Feasibility and comparison with conventional digital mammography and MR imaging in women with known breast carcinoma. *Radiology* **2013**, *266*, 743–751. [[CrossRef](#)]
50. Lee, S.; Lee, Y. Performance evaluation of total variation (TV) denoising technique for dual-energy contrast-enhanced digital mammography (CEDM) with photon counting detector (PCD): Monte Carlo simulation study. *Radiat. Phys. Chem.* **2019**, *156*, 94–100. [[CrossRef](#)]
51. Mori, M.; Akashi-Tanaka, S.; Suzuki, S.; Daniels, M.I.; Watanabe, C.; Hirose, M.; Nakamura, S. Diagnostic accuracy of contrast-enhanced spectral mammography in comparison to conventional full-field digital mammography in a population of women with dense breasts. *Breast Cancer* **2017**, *24*, 104–110. [[CrossRef](#)]
52. Kim, G.; Phillips, J.; Cole, E.; Brook, A.; Mehta, T.; Slanetz, P.; Fishman, M.D.C.; Karimova, E.; Mehta, R.; Lotfi, P.; et al. Comparison of Contrast-Enhanced Mammography With Conventional Digital Mammography in Breast Cancer Screening: A Pilot Study. *J. Am. Coll. Radiol.* **2019**, *16*, 1456–1463. [[CrossRef](#)]
53. Sorin, V.; Yagil, Y.; Yosepovich, A.; Shalmon, A.; Gotlieb, M.; Neiman, O.H.; Sklair-Levy, M. Contrast-enhanced spectral mammography in women with intermediate breast cancer risk and dense breasts. *AJR Am. J. Roentgenol.* **2018**, *211*, W267–W274. [[CrossRef](#)] [[PubMed](#)]
54. Sudhir, R.; Sannapareddy, K.; Potlapalli, A.; Krishnamurthy, P.B.; Buddha, S.; Koppula, V. Diagnostic accuracy of contrast-enhanced digital mammography in breast cancer detection in comparison to tomosynthesis, synthetic 2D mammography and tomosynthesis combined with ultrasound in women with dense breast. *Br. J. Radiol.* **2021**, *94*, 20201046. [[CrossRef](#)] [[PubMed](#)]
55. Li, L.; Roth, R.; Germaine, P.; Ren, S.; Lee, M.; Hunter, K.; Tinney, E.; Liao, L. Contrast-enhanced spectral mammography (CESM) versus breast magnetic resonance imaging (MRI): A retrospective comparison in 66 breast lesions. *Diagn. Interv. Imaging* **2017**, *98*, 113–123. [[CrossRef](#)] [[PubMed](#)]
56. Phillips, J.; Miller, M.M.; Mehta, T.S.; Fein-Zachary, V.; Nathanson, A.; Hori, W.; Monahan-Earley, R.; Slanetz, P.J. Contrast-enhanced spectral mammography (CESM) versus MRI in the high-risk screening setting: Patient preferences and attitudes. *Clin. Imaging* **2017**, *42*, 193–197. [[CrossRef](#)] [[PubMed](#)]
57. Bozzini, A.; Nicosia, L.; Pruneri, G.; Maisonneuve, P.; Meneghetti, L.; Renne, G.; Vingiani, A.; Cassano, E.; Mastropasqua, M.G. Clinical performance of contrast-enhanced spectral mammography in pre-surgical evaluation of breast malignant lesions in dense breasts: A single center study. *Breast Cancer Res. Treat.* **2020**, *184*, 723–731. [[CrossRef](#)] [[PubMed](#)]
58. Chou, C.-P.; Lewin, J.M.; Chiang, C.-L.; Hung, B.-H.; Yang, T.-L.; Huang, J.-S.; Liao, J.-B.; Pan, H.-B. Clinical evaluation of contrast-enhanced digital mammography and contrast enhanced tomosynthesis—Comparison to contrast-enhanced breast MRI. *Eur. J. Radiol.* **2015**, *84*, 2501–2508. [[CrossRef](#)]
59. Huang, J.-S.; Pan, H.-B.; Yang, T.-L.; Hung, B.-H.; Chiang, C.-L.; Tsai, M.-Y.; Chou, C.-P. Kinetic patterns of benign and malignant breast lesions on contrast enhanced digital mammogram. *PLoS ONE* **2020**, *15*, e0239271. [[CrossRef](#)]
60. De Silva, F.; Alcorn, J. A tale of two cancers: A current concise overview of breast and prostate cancer. *Cancers* **2022**, *14*, 2954. [[CrossRef](#)]
61. Hogan, M.P.; Horvat, J.V.; Ross, D.S.; Sevilimedu, V.; Jochelson, M.S.; Kirstein, L.J.; Goldfarb, S.B.; Comstock, C.E.; Sung, J.S. Contrast-enhanced mammography in the assessment of residual disease after neoadjuvant treatment. *Breast Cancer Res. Treat.* **2023**, *198*, 349–359. [[CrossRef](#)]
62. Bicchierai, G.; Tonelli, P.; Piacenti, A.; De Benedetto, D.; Boeri, C.; Vanzi, E.; Bianchi, S.; Cirone, D.; Kaur Gill, M.; Miele, V. Evaluation of contrast-enhanced digital mammography (CEDM) in the preoperative staging of breast cancer: Large-scale single-center experience. *Breast J.* **2020**, *26*, 1276–1283. [[CrossRef](#)]
63. Bicchierai, G.; Amato, F.; Vanzi, B.; De Benedetto, D.; Boeri, C.; Vanzi, E.; Di Naro, F.; Bianchi, S.; Cirone, D.; Cozzi, D. Which clinical, radiological, histological, and molecular parameters are associated with the absence of enhancement of known breast cancers with Contrast Enhanced Digital Mammography (CEDM)? *Breast* **2020**, *54*, 15–24. [[CrossRef](#)] [[PubMed](#)]
64. Patel, B.K.; Naylor, M.E.; Kosiorek, H.E.; Lopez-Alvarez, Y.M.; Miller, A.M.; Pizzitola, V.J.; Pockaj, B.A. Clinical utility of contrast-enhanced spectral mammography as an adjunct for tomosynthesis-detected architectural distortion. *Clin. Imaging* **2017**, *46*, 44–52. [[CrossRef](#)] [[PubMed](#)]
65. Naha, P.C.; Lau, K.C.; Hsu, J.C.; Hajfathalian, M.; Mian, S.; Chhour, P.; Uppuluri, L.; McDonald, E.S.; Maidment, A.D.; Cormode, D.P. Gold silver alloy nanoparticles (GSAN): An imaging probe for breast cancer screening with dual-energy mammography or computed tomography. *Nanoscale* **2016**, *8*, 13740–13754. [[CrossRef](#)] [[PubMed](#)]
66. Nieves, L.M.; Hsu, J.C.; Lau, K.C.; Maidment, A.D.; Cormode, D.P. Silver telluride nanoparticles as biocompatible and enhanced contrast agents for X-ray imaging: An in vivo breast cancer screening study. *Nanoscale* **2021**, *13*, 163–174. [[CrossRef](#)]
67. Karunamuni, R.; Naha, P.C.; Lau, K.C.; Al-Zaki, A.; Popov, A.V.; Delikatny, E.J.; Tsourkas, A.; Cormode, D.P.; Maidment, A.D. Development of silica-encapsulated silver nanoparticles as contrast agents intended for dual-energy mammography. *Eur. Radiol.* **2016**, *26*, 3301–3309. [[CrossRef](#)]
68. Cole, L.E.; Vargo-Gogola, T.; Roeder, R.K. Contrast-enhanced X-ray detection of breast microcalcifications in a murine model using targeted gold nanoparticles. *ACS Nano* **2014**, *8*, 7486–7496. [[CrossRef](#)]
69. Cole, L.E.; Vargo-Gogola, T.; Roeder, R.K. Contrast-enhanced x-ray detection of microcalcifications in radiographically dense mammary tissue using targeted gold nanoparticles. *ACS Nano* **2015**, *9*, 8923–8932. [[CrossRef](#)]

70. Choudhery, S.; Axmacher, J.; Conners, A.L.; Geske, J.; Brandt, K. Masses in the era of screening tomosynthesis: Is diagnostic ultrasound sufficient? *Br. J. Radiol.* **2019**, *92*, 20180801. [[CrossRef](#)]
71. Vourtsis, A.; Kachulis, A. The performance of 3D ABUS versus HHUS in the visualisation and BI-RADS characterisation of breast lesions in a large cohort of 1886 women. *Eur. Radiol.* **2018**, *28*, 592–601. [[CrossRef](#)]
72. Lin, X.; Wang, J.; Han, F.; Fu, J.; Li, A. Analysis of eighty-one cases with breast lesions using automated breast volume scanner and comparison with handheld ultrasound. *Eur. J. Radiol.* **2012**, *81*, 873–878. [[CrossRef](#)]
73. Shin, H.J.; Kim, H.H.; Cha, J.H. Current status of automated breast ultrasonography. *Ultrasonography* **2015**, *34*, 165. [[CrossRef](#)] [[PubMed](#)]
74. Melnikow, J.; Fenton, J.J.; Whitlock, E.P.; Miglioretti, D.L.; Weyrich, M.S.; Thompson, J.H.; Shah, K. Supplemental Screening for Breast Cancer in Women With Dense Breasts: A Systematic Review for the U.S. Preventive Services Task Force. *Ann. Intern. Med.* **2016**, *164*, 268–278. [[CrossRef](#)] [[PubMed](#)]
75. Lee, J.M.; Partridge, S.C.; Liao, G.J.; Hippe, D.S.; Kim, A.E.; Lee, C.I.; Rahbar, H.; Scheel, J.R.; Lehman, C.D. Double reading of automated breast ultrasound with digital mammography or digital breast tomosynthesis for breast cancer screening. *Clin. Imaging* **2019**, *55*, 119–125. [[CrossRef](#)] [[PubMed](#)]
76. Sood, R.; Rositch, A.F.; Shakoor, D.; Ambinder, E.; Pool, K.-L.; Pollack, E.; Mollura, D.J.; Mullen, L.A.; Harvey, S.C. Ultrasound for breast cancer detection globally: A systematic review and meta-analysis. *J. Glob. Oncol.* **2019**, *5*, 1–17. [[CrossRef](#)] [[PubMed](#)]
77. Badu-Peprah, A.; Adu-Sarkodie, Y. Accuracy of clinical diagnosis, mammography and ultrasonography in preoperative assessment of breast cancer. *Ghana Med. J.* **2018**, *52*, 133–139. [[CrossRef](#)] [[PubMed](#)]
78. Harada-Shoji, N.; Suzuki, A.; Ishida, T.; Zheng, Y.-F.; Narikawa-Shiono, Y.; Sato-Tadano, A.; Ohta, R.; Ohuchi, N. Evaluation of adjunctive ultrasonography for breast cancer detection among women aged 40–49 years with varying breast density undergoing screening mammography: A secondary analysis of a randomized clinical trial. *JAMA Netw. Open* **2021**, *4*, e2121505. [[CrossRef](#)] [[PubMed](#)]
79. Yi, A.; Jang, M.-j.; Yim, D.; Kwon, B.R.; Shin, S.U.; Chang, J.M. Addition of screening breast US to digital mammography and digital breast Tomosynthesis for breast cancer screening in women at average risk. *Radiology* **2021**, *298*, 568–575. [[CrossRef](#)]
80. Dibble, E.H.; Singer, T.M.; Jimoh, N.; Baird, G.L.; Lourenco, A.P. Dense Breast Ultrasound Screening After Digital Mammography Versus After Digital Breast Tomosynthesis. *Am. J. Roentgenol.* **2019**, *213*, 1397–1402. [[CrossRef](#)]
81. Choi, H.Y.; Park, M.; Seo, M.; Song, E.; Shin, S.Y.; Sohn, Y.-M. Preoperative axillary lymph node evaluation in breast cancer: Current issues and literature review. *Ultrasound Q.* **2017**, *33*, 6–14. [[CrossRef](#)]
82. Lu, Z.; Hao, C.; Pan, Y.; Mao, N.; Wang, X.; Yin, X. Contrast-enhanced spectral mammography versus ultrasonography: Diagnostic performance in symptomatic patients with dense breasts. *Korean J. Radiol.* **2020**, *21*, 442–449. [[CrossRef](#)]
83. Boyd, N.F.; Guo, H.; Martin, L.J.; Sun, L.; Stone, J.; Fishell, E.; Jong, R.A.; Hislop, G.; Chiarelli, A.; Minkin, S. Mammographic density and the risk and detection of breast cancer. *N. Engl. J. Med.* **2007**, *356*, 227–236. [[CrossRef](#)] [[PubMed](#)]
84. Thigpen, D.; Kappler, A.; Brem, R. The Role of Ultrasound in Screening Dense Breasts—A Review of the Literature and Practical Solutions for Implementation. *Diagnostics* **2018**, *8*, 20. [[CrossRef](#)]
85. Berg, W.A.; Gutierrez, L.; NessAiver, M.S.; Carter, W.B.; Bhargavan, M.; Lewis, R.S.; Ioffe, O.B. Diagnostic accuracy of mammography, clinical examination, US, and MR imaging in preoperative assessment of breast cancer. *Radiology* **2004**, *233*, 830–849. [[CrossRef](#)] [[PubMed](#)]
86. Teh, W.; Wilson, A. The role of ultrasound in breast cancer screening. A consensus statement by the European Group for Breast Cancer Screening. *Eur. J. Cancer* **1998**, *34*, 449–450. [[CrossRef](#)] [[PubMed](#)]
87. Iranmakani, S.; Mortezaazadeh, T.; Sajadian, F.; Ghaziani, M.F.; Ghafari, A.; Khezerloo, D.; Musa, A.E. A review of various modalities in breast imaging: Technical aspects and clinical outcomes. *Egypt. J. Radiol. Nucl. Med.* **2020**, *51*, 57. [[CrossRef](#)]
88. Shin, S.U.; Chang, J.M.; Park, J.; Lee, H.B.; Han, W.; Moon, W.K. The Usefulness of Ultrasound Surveillance for Axillary Recurrence in Women With Personal History of Breast Cancer. *J. Breast Cancer* **2022**, *25*, 25–36. [[CrossRef](#)] [[PubMed](#)]
89. Kim, S.-Y.; Cho, N.; Kim, S.Y.; Choi, Y.; Kim, E.S.; Ha, S.M.; Lee, S.H.; Chang, J.M.; Moon, W.K. Supplemental Breast US Screening in Women with a Personal History of Breast Cancer: A Matched Cohort Study. *Radiology* **2020**, *295*, 54–63. [[CrossRef](#)] [[PubMed](#)]
90. Tan-Chiu, E.; Wang, J.; Costantino, J.P.; Paik, S.; Butch, C.; Wickerham, D.L.; Fisher, B.; Wolmark, N. Effects of tamoxifen on benign breast disease in women at high risk for breast cancer. *J. Natl. Cancer Inst.* **2003**, *95*, 302–307. [[CrossRef](#)] [[PubMed](#)]
91. Milgroom, A.; Intrator, M.; Madhavan, K.; Mazzaro, L.; Shandas, R.; Liu, B.; Park, D. Mesoporous silica nanoparticles as a breast-cancer targeting ultrasound contrast agent. *Colloids Surf. B Biointerfaces* **2014**, *116*, 652–657. [[CrossRef](#)]
92. Subhan, M.A. Advances with metal oxide-based nanoparticles as MDR metastatic breast cancer therapeutics and diagnostics. *RSC Adv.* **2022**, *12*, 32956–32978. [[CrossRef](#)]
93. Nguyen Cao, T.G.; Kang, J.H.; You, J.Y.; Kang, H.C.; Rhee, W.J.; Ko, Y.T.; Shim, M.S. Safe and Targeted Sonodynamic Cancer Therapy Using Biocompatible Exosome-Based Nanosensitizers. *ACS Appl. Mater. Interfaces* **2021**, *13*, 25575–25588. [[CrossRef](#)] [[PubMed](#)]
94. Morrow, M.; Waters, J.; Morris, E. MRI for breast cancer screening, diagnosis, and treatment. *Lancet* **2011**, *378*, 1804–1811. [[CrossRef](#)] [[PubMed](#)]
95. Daly, M.B.; Pilarski, R.; Berry, M.; Buys, S.S.; Farmer, M.; Friedman, S.; Garber, J.E.; Kauff, N.D.; Khan, S.; Klein, C. NCCN guidelines insights: Genetic/familial high-risk assessment: Breast and ovarian, version 2.2017. *J. Natl. Compr. Cancer Netw.* **2017**, *15*, 9–20. [[CrossRef](#)] [[PubMed](#)]

96. Gradishar, W.J.; Anderson, B.O.; Balassanian, R.; Blair, S.L.; Burstein, H.J.; Cyr, A.; Elias, A.D.; Farrar, W.B.; Forero, A.; Giordano, S.H.; et al. NCCN Guidelines Insights: Breast Cancer, Version 1.2017. *J. Natl. Compr. Cancer Netw. JNCCN* **2017**, *15*, 433–451. [[CrossRef](#)] [[PubMed](#)]
97. Riedl, C.C.; Luft, N.; Bernhart, C.; Weber, M.; Bernathova, M.; Tea, M.K.; Rudas, M.; Singer, C.F.; Helbich, T.H. Triple-modality screening trial for familial breast cancer underlines the importance of magnetic resonance imaging and questions the role of mammography and ultrasound regardless of patient mutation status, age, and breast density. *J. Clin. Oncol. Off. J. Am. Soc. Clin. Oncol.* **2015**, *33*, 1128–1135. [[CrossRef](#)] [[PubMed](#)]
98. Benndorf, M.; Baltzer, P.A.; Vag, T.; Gajda, M.; Runnebaum, I.B.; Kaiser, W.A. Breast MRI as an adjunct to mammography: Does it really suffer from low specificity? A retrospective analysis stratified by mammographic BI-RADS classes. *Acta Radiol.* **2010**, *51*, 715–721. [[CrossRef](#)] [[PubMed](#)]
99. Kaiser, C.G.; Dietzel, M.; Vag, T.; Froelich, M.F. Cost-effectiveness of MR-mammography vs. conventional mammography in screening patients at intermediate risk of breast cancer—A model-based economic evaluation. *Eur. J. Radiol.* **2021**, *136*, 109355. [[CrossRef](#)]
100. Sippo, D.A.; Burk, K.S.; Mercaldo, S.F.; Rutledge, G.M.; Edmonds, C.; Guan, Z.; Hughes, K.S.; Lehman, C.D. Performance of screening breast MRI across women with different elevated breast cancer risk indications. *Radiology* **2019**, *292*, 51–59. [[CrossRef](#)]
101. Kim, S.-Y.; Cho, N.; Hong, H.; Lee, Y.; Yoen, H.; Kim, Y.S.; Park, A.R.; Ha, S.M.; Lee, S.H.; Chang, J.M.; et al. Abbreviated Screening MRI for Women with a History of Breast Cancer: Comparison with Full-Protocol Breast MRI. *Radiology* **2022**, *305*, 36–45. [[CrossRef](#)]
102. Plana, M.N.; Carreira, C.; Muriel, A.; Chiva, M.; Abaira, V.; Emparanza, J.I.; Bonfill, X.; Zamora, J. Magnetic resonance imaging in the preoperative assessment of patients with primary breast cancer: Systematic review of diagnostic accuracy and meta-analysis. *Eur. Radiol.* **2012**, *22*, 26–38. [[CrossRef](#)]
103. Comstock, C.E.; Gatsonis, C.; Newstead, G.M.; Snyder, B.S.; Gareen, I.F.; Bergin, J.T.; Rahbar, H.; Sung, J.S.; Jacobs, C.; Harvey, J.A.; et al. Comparison of Abbreviated Breast MRI vs Digital Breast Tomosynthesis for Breast Cancer Detection among Women With Dense Breasts Undergoing Screening. *JAMA* **2020**, *323*, 746–756. [[CrossRef](#)]
104. Vreemann, S.; van Zelst, J.C.M.; Schlooz-Vries, M.; Bult, P.; Hoogerbrugge, N.; Karssemeijer, N.; Gubern-Mérida, A.; Mann, R.M. The added value of mammography in different age-groups of women with and without BRCA mutation screened with breast MRI. *Breast Cancer Res.* **2018**, *20*, 84. [[CrossRef](#)]
105. Gu, W.Q.; Cai, S.M.; Liu, W.D.; Zhang, Q.; Shi, Y.; Du, L.J. Combined molybdenum target X-ray and magnetic resonance imaging examinations improve breast cancer diagnostic efficacy. *World J. Clin. Cases* **2022**, *10*, 485–491. [[CrossRef](#)]
106. Wernli, K.J.; Ichikawa, L.; Kerlikowske, K.; Buist, D.S.M.; Brandzel, S.D.; Bush, M.; Johnson, D.; Henderson, L.M.; Nekhlyudov, L.; Onega, T.; et al. Surveillance Breast MRI and Mammography: Comparison in Women with a Personal History of Breast Cancer. *Radiology* **2019**, *292*, 311–318. [[CrossRef](#)]
107. Xiang, W.; Rao, H.; Zhou, L. A meta-analysis of contrast-enhanced spectral mammography versus MRI in the diagnosis of breast cancer. *Thorac. Cancer* **2020**, *11*, 1423–1432. [[CrossRef](#)]
108. Covington, M.F.; Pizzitola, V.J.; Lorans, R.; Pockaj, B.A.; Northfelt, D.W.; Appleton, C.M.; Patel, B.K. The future of contrast-enhanced mammography. *Am. J. Roentgenol.* **2018**, *210*, 292–300. [[CrossRef](#)]
109. Shahbazi-Gahrouei, D.; Aminolroayaei, F.; Nematollahi, H.; Ghaderian, M.; Shahbazi Gahrouei, S. Advanced magnetic resonance imaging modalities for breast cancer diagnosis: An overview of recent findings and perspectives. *Diagnostics* **2022**, *12*, 2741. [[CrossRef](#)]
110. Kaiser, C.G.; Dietzel, M.; Vag, T.; Rübenthaler, J.; Froelich, M.F.; Tollens, F. Impact of specificity on cost-effectiveness of screening women at high risk of breast cancer with magnetic resonance imaging, mammography and ultrasound. *Eur. J. Radiol.* **2021**, *137*, 109576. [[CrossRef](#)]
111. Graeser, M.; Schradung, S.; Gluz, O.; Strobel, K.; Herzog, C.; Umutlu, L.; Frydrychowicz, A.; Rjosk-Dendorfer, D.; Würstlein, R.; Culemann, R. Magnetic resonance imaging and ultrasound for prediction of residual tumor size in early breast cancer within the ADAPT subtrials. *Breast Cancer Res.* **2021**, *23*, 36. [[CrossRef](#)]
112. Romeo, V.; Helbich, T.H.; Pinker, K. Breast PET/MRI Hybrid imaging and targeted tracers. *J. Magn. Reson. Imaging* **2023**, *57*, 370–386. [[CrossRef](#)] [[PubMed](#)]
113. Morawitz, J.; Bruckmann, N.-M.; Dietzel, F.; Ullrich, T.; Bittner, A.-K.; Hoffmann, O.; Ruckhäberle, E.; Mohrmann, S.; Häberle, L.; Ingenwerth, M. Comparison of nodal staging between CT, MRI, and [18 F]-FDG PET/MRI in patients with newly diagnosed breast cancer. *Eur. J. Nucl. Med. Mol. Imaging* **2022**, *49*, 992–1001. [[CrossRef](#)]
114. Choi, E.J.; Choi, H.; Choi, S.A.; Youk, J.H. Dynamic contrast-enhanced breast magnetic resonance imaging for the prediction of early and late recurrences in breast cancer. *Medicine* **2016**, *95*, e5330. [[CrossRef](#)]
115. Amornsiripanitch, N.; Bickelhaupt, S.; Shin, H.J.; Dang, M.; Rahbar, H.; Pinker, K.; Partridge, S.C. Diffusion-weighted MRI for unenhanced breast cancer screening. *Radiology* **2019**, *293*, 504. [[CrossRef](#)]
116. Millet, I.; Pages, E.; Hoa, D.; Merigeaud, S.; Curros Doyon, F.; Prat, X.; Taourel, P. Pearls and pitfalls in breast MRI. *Br. J. Radiol.* **2012**, *85*, 197–207. [[CrossRef](#)]
117. Gulani, V.; Calamante, F.; Shellock, F.G.; Kanal, E.; Reeder, S.B. Gadolinium deposition in the brain: Summary of evidence and recommendations. *Lancet Neurol.* **2017**, *16*, 564–570. [[CrossRef](#)]



118. Layne, K.A.; Dargan, P.I.; Archer, J.R.; Wood, D.M. Gadolinium deposition and the potential for toxicological sequelae—A literature review of issues surrounding gadolinium-based contrast agents. *Br. J. Clin. Pharmacol.* **2018**, *84*, 2522–2534. [[CrossRef](#)]
119. Sharma, U.; Agarwal, K.; Hari, S.; Mathur, S.R.; Seenu, V.; Parshad, R.; Jagannathan, N.R. Role of diffusion weighted imaging and magnetic resonance spectroscopy in breast cancer patients with indeterminate dynamic contrast enhanced magnetic resonance imaging findings. *Magn. Reson. Imaging* **2019**, *61*, 66–72. [[CrossRef](#)]
120. Chotai, N.; Kulkarni, S. *Breast Imaging Essentials*; Springer: Berlin/Heidelberg, Germany, 2020.
121. Suh, J.; Kim, J.-H.; Kim, S.-Y.; Cho, N.; Kim, D.-H.; Kim, R.; Kim, E.S.; Jang, M.-j.; Ha, S.M.; Lee, S.H.; et al. Noncontrast-Enhanced MR-Based Conductivity Imaging for Breast Cancer Detection and Lesion Differentiation. *J. Magn. Reson. Imaging* **2021**, *54*, 631–645. [[CrossRef](#)] [[PubMed](#)]
122. Marino, M.A.; Leithner, D.; Sung, J.; Avendano, D.; Morris, E.A.; Pinker, K.; Jochelson, M.S. Radiomics for tumor characterization in breast cancer patients: A feasibility study comparing contrast-enhanced mammography and magnetic resonance imaging. *Diagnostics* **2020**, *10*, 492. [[CrossRef](#)] [[PubMed](#)]
123. Kamal, R.; Mansour, S.; Farouk, A.; Hanafy, M.; Elhatw, A.; Goma, M.M. Contrast-enhanced mammography in comparison with dynamic contrast-enhanced MRI: Which modality is appropriate for whom? *Egypt. J. Radiol. Nucl. Med.* **2021**, *52*, 216. [[CrossRef](#)]
124. Pötsch, N.; Vatteroni, G.; Clauser, P.; Helbich, T.H.; Baltzer, P.A. Contrast-enhanced mammography versus contrast-enhanced breast MRI: A systematic review and meta-analysis. *Radiology* **2022**, *305*, 94–103. [[CrossRef](#)] [[PubMed](#)]
125. Mann, R.M.; Kuhl, C.K.; Moy, L. Contrast-enhanced MRI for breast cancer screening. *J. Magn. Reson. Imaging* **2019**, *50*, 377–390. [[CrossRef](#)]
126. Barkhausen, J.; Bischof, A.; Haverstock, D.; Klemens, M.; Brueggenwerth, G.; Weber, O.; Endrikat, J. Diagnostic efficacy of contrast-enhanced breast MRI versus X-ray mammography in women with different degrees of breast density. *Acta Radiol.* **2021**, *62*, 586–593. [[CrossRef](#)]
127. Woitek, R.; McLean, M.A.; Gill, A.B.; Grist, J.T.; Provenzano, E.; Patterson, A.J.; Ursprung, S.; Torheim, T.; Zaccagna, F.; Locke, M.; et al. Hyperpolarized <sup>13</sup>C MRI of Tumor Metabolism Demonstrates Early Metabolic Response to Neoadjuvant Chemotherapy in Breast Cancer. *Radiol. Imaging Cancer* **2020**, *2*, e200017. [[CrossRef](#)]
128. Moy, L.; Noz, M.E.; Maguire Jr, G.Q.; Melsaether, A.; Deans, A.E.; Murphy-Walcott, A.D.; Ponzio, F. Role of fusion of prone FDG-PET and magnetic resonance imaging of the breasts in the evaluation of breast cancer. *Breast J.* **2010**, *16*, 369–376. [[CrossRef](#)]
129. Rabasco, P.; Caivano, R.; Simeon, V.; Dinardo, G.; Lotumolo, A.; Gioioso, M.; Villonio, A.; Iannelli, G.; D’Antuono, F.; Zandolino, A. Can diffusion-weighted imaging and related apparent diffusion coefficient be a prognostic value in women with breast cancer? *Cancer Investig.* **2017**, *35*, 92–99. [[CrossRef](#)]
130. Surov, A.; Meyer, H.J.; Wienke, A. Can apparent diffusion coefficient (ADC) distinguish breast cancer from benign breast findings? A meta-analysis based on 13 847 lesions. *BMC Cancer* **2019**, *19*, 955. [[CrossRef](#)]
131. Sharma, U.; Jagannathan, N.R. Characterization of breast tissues by diffusion weighted MR imaging. *Biomed. Spectrosc. Imaging* **2014**, *3*, 1–13. [[CrossRef](#)]
132. Pinker, K.; Moy, L.; Sutton, E.J.; Mann, R.M.; Weber, M.; Thakur, S.B.; Jochelson, M.S.; Bago-Horvath, Z.; Morris, E.A.; Baltzer, P.A. Diffusion-weighted imaging with apparent diffusion coefficient mapping for breast cancer detection as a stand-alone-parameter: Comparison with dynamic contrast-enhanced and multiparametric magnetic resonance imaging. *Investig. Radiol.* **2018**, *53*, 587. [[CrossRef](#)] [[PubMed](#)]
133. Cho, E.; Lee, J.H.; Baek, H.J.; Ha, J.Y.; Ryu, K.H.; Park, S.E.; Moon, J.I.; Gho, S.-M.; Wakayama, T. Clinical Feasibility of Reduced Field-of-View Diffusion-Weighted Magnetic Resonance Imaging with Computed Diffusion-Weighted Imaging Technique in Breast Cancer Patients. *Diagnostics* **2020**, *10*, 538. [[CrossRef](#)] [[PubMed](#)]
134. Partridge, S.C.; Nissan, N.; Rahbar, H.; Kitsch, A.E.; Sigmund, E.E. Diffusion-weighted breast MRI: Clinical applications and emerging techniques. *J. Magn. Reson. Imaging JMRI* **2017**, *45*, 337–355. [[CrossRef](#)] [[PubMed](#)]
135. Galati, F.; Trimboli, R.M.; Pediconi, F. Special Issue &ldquo;Advances in Breast MRI&rdquo;. *Diagnostics* **2021**, *11*, 2297. [[PubMed](#)]
136. Montemezzi, S.; Cavedon, C.; Camera, L.; Meliador, G.; Caumo, F.; Baglio, I.; Sardanelli, F. 1H-MR spectroscopy of suspicious breast mass lesions at 3T: A clinical experience. *La Radiol. Medica* **2017**, *122*, 161–170. [[CrossRef](#)] [[PubMed](#)]
137. Prvulovic Bunovic, N.; Sveljo, O.; Kozic, D.; Boban, J. Is Elevated Choline on Magnetic Resonance Spectroscopy a Reliable Marker of Breast Lesion Malignancy? *Front. Oncol.* **2021**, *11*, 610354. [[CrossRef](#)] [[PubMed](#)]
138. Sodano, C.; Clauser, P.; Dietzel, M.; Kapetas, P.; Pinker, K.; Helbich, T.H.; Gussew, A.; Baltzer, P.A. Clinical relevance of total choline (tCho) quantification in suspicious lesions on multiparametric breast MRI. *Eur. Radiol.* **2020**, *30*, 3371–3382. [[CrossRef](#)] [[PubMed](#)]
139. Hawley, J.R.; Kalra, P.; Mo, X.; Raterman, B.; Yee, L.D.; Kolipaka, A. Quantification of breast stiffness using MR elastography at 3 Tesla with a soft sternal driver: A reproducibility study. *J. Magn. Reson. Imaging JMRI* **2017**, *45*, 1379–1384. [[CrossRef](#)]
140. Patel, B.K.; Samreen, N.; Zhou, Y.; Chen, J.; Brandt, K.; Ehman, R.; Pepin, K. MR Elastography of the Breast: Evolution of Technique, Case Examples, and Future Directions. *Clin. Breast Cancer* **2021**, *21*, e102–e111. [[CrossRef](#)]
141. Pepin, K.M.; Ehman, R.L.; McGee, K.P. Magnetic resonance elastography (MRE) in cancer: Technique, analysis, and applications. *Prog. Nucl. Magn. Reson. Spectrosc.* **2015**, *90*, 32–48. [[CrossRef](#)]
142. Lorenzen, J.; Sinkus, R.; Lorenzen, M.; Dargatz, M.; Leussler, C.; Röschmann, P.; Adam, G. MR elastography of the breast: preliminary clinical results. *Rofo* **2002**, *174*, 830–834. [[CrossRef](#)]

143. Liu, L.; Yin, B.; Geng, D.Y.; Lu, Y.P.; Peng, W.J. Changes of T2 relaxation time from neoadjuvant chemotherapy in breast cancer lesions. *Iran. J. Radiol.* **2016**, *13*, e24014. [[CrossRef](#)]
144. Seo, M.; Ryu, J.K.; Jahng, G.-H.; Sohn, Y.-M.; Rhee, S.J.; Oh, J.-H.; Won, K.-Y. Estimation of T2\* relaxation time of breast cancer: Correlation with clinical, imaging and pathological features. *Korean J. Radiol.* **2017**, *18*, 238–248. [[CrossRef](#)] [[PubMed](#)]
145. Liu, L.; Yin, B.; Shek, K.; Geng, D.; Lu, Y.; Wen, J.; Kuai, X.; Peng, W. Role of quantitative analysis of T2 relaxation time in differentiating benign from malignant breast lesions. *J. Int. Med. Res.* **2018**, *46*, 1928–1935. [[CrossRef](#)] [[PubMed](#)]
146. Meng, T.; He, N.; He, H.; Liu, K.; Ke, L.; Liu, H.; Zhong, L.; Huang, C.; Yang, A.; Zhou, C. The diagnostic performance of quantitative mapping in breast cancer patients: A preliminary study using synthetic MRI. *Cancer Imaging* **2020**, *20*, 88. [[CrossRef](#)] [[PubMed](#)]
147. Salimi, M.; Sarkar, S.; Saber, R.; Delavari, H.; Alizadeh, A.M.; Mulder, H.T. Magnetic hyperthermia of breast cancer cells and MRI relaxometry with dendrimer-coated iron-oxide nanoparticles. *Cancer Nanotechnol* **2018**, *9*, 7. [[CrossRef](#)] [[PubMed](#)]
148. Núñez, C.; Estévez, S.V.; del Pilar Chantada, M. Inorganic nanoparticles in diagnosis and treatment of breast cancer. *JBIC J. Biol. Inorg. Chem.* **2018**, *23*, 331–345. [[CrossRef](#)] [[PubMed](#)]
149. Jeon, M.; Halbert, M.V.; Stephen, Z.R.; Zhang, M. Iron Oxide Nanoparticles as T(1) Contrast Agents for Magnetic Resonance Imaging: Fundamentals, Challenges, Applications, and Prospectives. *Adv. Mater.* **2021**, *33*, e1906539. [[CrossRef](#)]
150. Xiao, S.; Yu, X.; Zhang, L.; Zhang, Y.; Fan, W.; Sun, T.; Zhou, C.; Liu, Y.; Liu, Y.; Gong, M.; et al. Synthesis Of PEG-Coated, Ultrasmall, Manganese-Doped Iron Oxide Nanoparticles With High Relaxivity For T(1)/T(2) Dual-Contrast Magnetic Resonance Imaging. *Int. J. Nanomed.* **2019**, *14*, 8499–8507. [[CrossRef](#)]
151. Huang, H.; Yue, T.; Xu, K.; Golzarian, J.; Yu, J.; Huang, J. Fabrication and evaluation of tumor-targeted positive MRI contrast agent based on ultrasmall MnO nanoparticles. *Colloids Surf. B Biointerfaces* **2015**, *131*, 148–154. [[CrossRef](#)]
152. Ye, Y.J.; Huang, X.J.; Luo, B.C.; Wang, X.Y.; Cai, X.R. Application of multiparametric magnetic resonance imaging to monitor the early antitumor effect of CuS@GOD nanoparticles in a 4 T1 breast cancer xenograft model. *J. Magn. Reson. Imaging* **2022**, *55*, 301–310. [[CrossRef](#)]
153. Tao, Y.; Li, Y.; Wei, D.; Liang, M.; Ren, P.; Dai, J.; Zhang, T.; Lei, J.; Liu, P. Fe3O4 Nanoparticles Embedded in Pectin–Doxorubicin Composites as pH-Responsive Nanoplatfoms for Tumor Diagnosis and Therapy by T1-Weighted Magnetic Imaging. *ACS Appl. Nano Mater.* **2022**, *6*, 633–645. [[CrossRef](#)]
154. Cheng, K.; Peng, S.; Xu, C.; Sun, S. Porous hollow Fe3O4 nanoparticles for targeted delivery and controlled release of cisplatin. *J. Am. Chem. Soc.* **2009**, *131*, 10637–10644. [[CrossRef](#)] [[PubMed](#)]
155. Lee, J.E.; Lee, N.; Kim, H.; Kim, J.; Choi, S.H.; Kim, J.H.; Kim, T.; Song, I.C.; Park, S.P.; Moon, W.K. Uniform mesoporous dye-doped silica nanoparticles decorated with multiple magnetite nanocrystals for simultaneous enhanced magnetic resonance imaging, fluorescence imaging, and drug delivery. *J. Am. Chem. Soc.* **2010**, *132*, 552–557. [[CrossRef](#)] [[PubMed](#)]
156. Ramalho, J.; Semelka, R.; Ramalho, M.; Nunes, R.; AlObaidy, M.; Castillo, M. Gadolinium-based contrast agent accumulation and toxicity: An update. *Am. J. Neuroradiol.* **2016**, *37*, 1192–1198. [[CrossRef](#)] [[PubMed](#)]
157. Choi, H.S.; Liu, W.; Liu, F.; Nasr, K.; Misra, P.; Bawendi, M.G.; Frangioni, J.V. Design considerations for tumour-targeted nanoparticles. *Nat. Nanotechnol.* **2010**, *5*, 42–47. [[CrossRef](#)]
158. Rogosnitzky, M.; Branch, S. Gadolinium-based contrast agent toxicity: A review of known and proposed mechanisms. *Biometals* **2016**, *29*, 365–376. [[CrossRef](#)]
159. Poplack, S.P.; Park, E.-Y.; Ferrara, K.W. Optical breast imaging: A review of physical principles, technologies, and clinical applications. *J. Breast Imaging* **2023**, *5*, 520–537. [[CrossRef](#)]

**Disclaimer/Publisher’s Note:** The statements, opinions and data contained in all publications are solely those of the individual author(s) and contributor(s) and not of MDPI and/or the editor(s). MDPI and/or the editor(s) disclaim responsibility for any injury to people or property resulting from any ideas, methods, instructions or products referred to in the content.